Eur. Phys. J. A **21**, 193–215 (2004)
DOI 10.1140/epja/i2003-10188-9

THE EUROPEAN PHYSICAL JOURNAL A

Search for cluster structure of excited states in ^{14}C

W. von Oertzen[1,2,a], H.G. Bohlen[2], M. Milin[1,2,3], Tz. Kokalova[1,2], S. Thummerer[2], A. Tumino[1,2,4], R. Kalpakchieva[5], T.N. Massey[6], Y. Eisermann[7], G. Graw[7], T. Faestermann[8], R. Hertenberger[7], and H.-F. Wirth[7]

[1] Freie Universität Berlin, Fachbereich Physik, Arnimallee 14, D-14195 Berlin, Germany
[2] Hahn-Meitner-Institut Berlin, Glienicker Strasse 100, D-14109 Berlin, Germany
[3] Ruđer Bošković Institute, P.O. Box 180, HR-10002 Zagreb, Croatia
[4] INFN-Laboratori Nazionali del Sud and Università di Catania, Via S. Sofia 44, I-95123 Catania, Italy
[5] Flerov Laboratory of Nuclear Reactions, JINR, RU-141980 Dubna, Russia and Institute for Nuclear Research and Nuclear Energy, BAS, BG-1784 Sofia, Bulgaria
[6] Department of Physics and Astronomy, Ohio University, Athens, OH 45701-2979, USA
[7] Sektion Physik der Universität München, Am Coulombwall 1, D-85748 Garching, Germany
[8] Technische Universität München, Am Coulombwall 1, D-85748 Garching, Germany

Received: 3 November 2003 / Revised version: 23 December 2003 /
Published online: 24 August 2004 –
Communicated by J. Äystö

Abstract. We have studied three different 2n-transfer reactions on a ^{12}C target, the 2p pick-up reaction on ^{16}O and the ^{5}He transfer in the reaction ^{9}Be(^{7}Li, d)^{14}C. Combined with a systematic search through experimental results for transfer reactions, inelastic excitations and other data, we have established an almost complete spectroscopy for ^{14}C up to 18 MeV excitation. We identify states with single-particle structure that have oblate shapes and states corresponding to proton excitations that are connected to oblate (triangular) cluster states. Further we list states of prolate shape which have no simple structure related to the low-lying oblate states of ^{12}C. These are proposed to have strong α-clustering and to form rotational bands as a parity inversion doublet, with high moment of inertia. With these results it is possible for the first time to identify chain states expected in the isotope ^{14}C.

PACS. 21.10.-k Properties of nuclei; nuclear energy levels – 21.60.Gx Cluster models

1 Introduction

Neutron-rich carbon isotopes are expected to show specific features in excited states, which can be related to strong α-particle clustering. The observation of unique deformed shapes like α-cluster chains or triangles, discussed in $N = Z$ α-cluster nuclei is also expected at high excitation energies in neutron-rich nuclei [1–10]. These features are related to neutron molecular orbitals established for certain structures in excited states of $^{9-12}$Be isotopes. Such structures are based on the particular property of the $\alpha + \alpha$ potential: the local potential is very shallow (slightly attractive) and has a strong repulsion at small distances. This repulsion is due to the effect of the Pauli blocking: in the case of two α-clusters the nucleons of the second cluster have to move up into the next major shell at smaller distances. This fact is responsible for the molecular shape of the $\alpha + \alpha$ potential and makes the ground state of ^{8}Be a clear $l = 0$ resonance at a very low energy $E_\alpha^{\rm cm} = 92$ keV. The higher rotational excitations, the 2^+ and 4^+ states are well known.

In the framework of nuclear structure with deformation we start from the ^{8}Be nucleus as the first "superdeformed" nucleus (a nucleus with a 2 : 1 deformation). In fig. 1 a survey of the energy splitting of orbitals in an axially symmetric deformed nucleus (harmonic oscillator) is shown. According to this diagram we can form stable shapes with two choices of deformed shells, they can be arranged in a energetically favored prolate configuration (deformation with axis ratios 2 : 1, 3 : 1 and higher) or oblate configurations (with axis ratio 1 : 2). The latter correspond to specific arrangements in which local energy minima are achieved for the three α-particles. In the discussion of excited states of $^{12-16}$C both configurations must be considered. The diagram shown in fig. 1 allows also to discuss the properties of the first valence particle orbits on top of a deformed shell structure.

The nucleus ^{8}Be is also the starting point of the Ikeda diagram of cluster nuclei [2]. An extension to covalently bound nuclear cluster structures can be obtained by adding covalent neutrons and thus a new threshold

[a] e-mail: oertzen@hmi.de

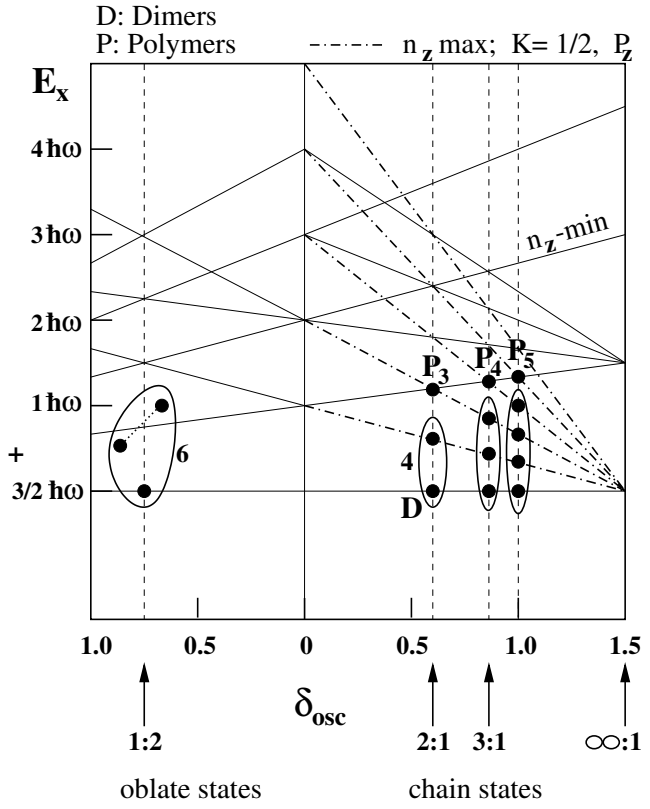

Fig. 1. Diagram of energy levels in a deformed harmonic oscillator, and the related shells for axially symmetric shapes; the first "magic" numbers for protons and neutrons in prolate configurations related to chain states are emphasized. P_i indicates stable configurations with particular degeneracy, where i is the number of α-particles in a chain. On the left side (with oblate states) 6 nucleons in the first 2 orbits form a triangular structure. Some orbits are labeled by the number of nodes, n_z in the z-axis. The energy is counted from the lowest level $(3/2\hbar)$ in units of harmonic-oscillator energies. Places where oblate quadrupole ($\delta < 0$) and prolate ($\delta > 0$) deformations occur are indicated (adapted from ref. [11]).

diagram results [12]. The formation of covalently bound molecular structures relies not only on certain properties of the core-core potential but also on particular properties of the nucleonic molecular orbitals, which for the $\alpha+\alpha+$n system are now well studied [1,6,13–15]. Due to the high binding energy of the α-clusters ($\approx 24\,$MeV), and due to the very weak binding of the next neutron (which is in a $p_{3/2}$-resonance in ^{5}He), the concept of molecular orbitals for neutrons appears particularly attractive. Therefore in systems with α-clusters the valence particle can be well separated from the core.

Thus, a variety of cluster models and molecular orbital models have been applied to weakly bound nuclei. For the description of covalently bound molecules in nuclear physics the effects of antisymmetrisation are often neglected. These effects are, if necessary, reflected in reduced spectroscopic factors (*i.e.* values below the shell model limit). The same argument to neglect antisymmetrisation would be valid for the core-core interactions, as long as the distance between the cores remains large and the *local potential becomes strongly repulsive* at smaller distances. This behavior is in close analogy with that of valence particles in atomic molecules, where no antisymmetrisation between valence particles and the cores is needed. In this sense the molecular orbital approach defines a different limit, when compared, for example, to the generator coordinate methods [16], where the antisymmetrisation of all nucleons is introduced at the very beginning (into the total wave functions).

The present paper is organized as follows. Models for molecular configurations in ^{14}C are discussed in sect. 2; in sect. 3 results from our own recent experiments are reported and the information is combined with results from a variety of reactions from the literature. This is followed (sect. 4) by a survey of known states grouped into rotational bands (including previously published experimental results). In sect. 5 we give a discussion of the present result in its relation to cluster and polymer structures expected in the isotopes in $^{13-16}$C.

After the first study of cluster structure in carbon isotopes with molecular orbitals for the case of ^{13}C [8,9], we look in the present work to the possible evidence for molecular structure in ^{14}C. We try to make a complete spectroscopy for ^{14}C, first by identifying the states with single-particle properties and by "removing" these states with mostly single-particle neutron excitations. We expect the remaining states to be more strongly deformed and to form the rotational bands based on cluster states related to the $^{10}\mathrm{Be}+\alpha$ structure.

The most useful in the determination of states with firm spin/parity assignments at high excitation energies are the reactions involving pions. The (p,π) reaction [17, 18] on ^{13}C is very selective to high-spin states of negative parity. A very strong peak observed in ref. [18] is identified as a 5^- state at 14.87 MeV. Similarly inelastic and charge exchange reactions involving ^{14}C targets have yielded unique information.

In our recent experiments on multi-nucleon transfer and in some of the reactions from the literature many more states at higher excitation are observed, which we have not placed in the present band structures. Several of them are candidates for molecular configurations with more extended α-n-α-n-α structure, which will be discussed elsewhere [19]. Discussions, comparison with other work and conclusions are given in sect. 5.

2 Models for molecular configurations in ^{14}C

The structure of molecular states in ^{14}C is strongly related to the structure in the dimers of the beryllium isotopes, where the concepts of molecular orbitals have been applied [1,14,15,20].

The nuclear molecular orbital model for dimers is related to the two-centre shell model (TCSM) [21]. There, however, not only valence nucleons, but all nucleons are considered. A calculated correlation diagram from

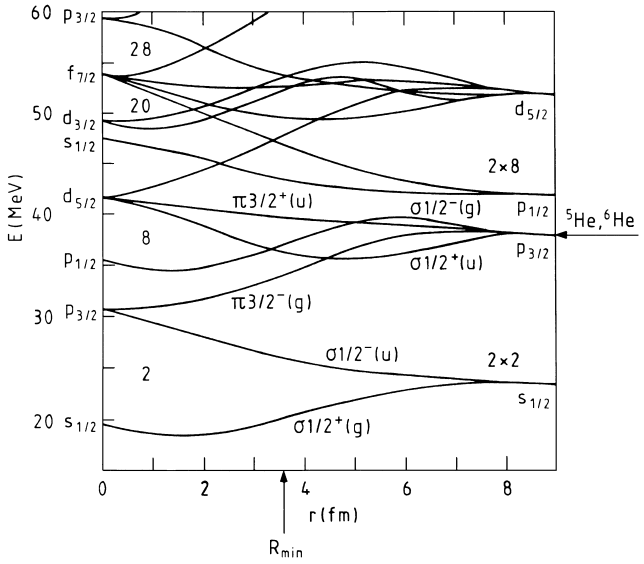

Fig. 2. Correlation diagram of molecular orbitals in a two-centre shell model picture [1,21]. The orbitals are labeled by their quantum numbers. The position of the $p_{3/2}$ neutron orbital in $^{5-6}$He is indicated. The distance between the two centres is $\mathtt{r}$, the arrow indicates the distance where the minimum in the α-α potential occurs.

ref. [21], shown in fig. 2, can be interpreted in analogy to the well-known correlation diagrams of atomic physics (see, for example, ref. [22], p. 328).

The two-centre correlation diagram merges at small distances with the Nilsson diagram of the deformed compound nucleus. Due to the axial symmetry, projections on the z-axis appear as conserved quantum numbers. The molecular configurations are classified according to the well-known quantum numbers of axial symmetric molecular states: the K-quantum number for the projection of the spin on the symmetry axis, the σ and π orbitals for the $m_l = 0$ and $m_l = 1$ projections of the orbital angular momentum, the parity, π, and the *gerade* (g) and *ungerade* (u) symmetry due to the identity of the two molecular cores; the latter two are related by $\pi = (-)^l$ $(\text{-})^p$, with l the angular momentum of the nucleon in the separated centres, and the phase factor $(\text{-})^p = +/-$, for g and u, respectively.

With the correlation diagram we are able to discuss [1] the structure of all states of the neutron-rich isotopes $^{9-12}$Be, by considering the occupation of the molecular orbitals for an α-α distance corresponding to the potential minimum, or to a deformation in the Nilsson model with a value of the parameter $\beta_2 \approx 0.6$. In a variety of recent experiments using stable [23–28] and radioactive [29–31] beams, such strongly deformed structures of states in beryllium isotopes have been established; a recent compilation of the data is given in refs. [25,28].

Adding a third α-particle to the Be dimers we have to consider for the *carbon isotopes* both, oblate shapes with triangular configurations and prolate shapes with linear configurations of the three α-particles. Such structures have been recently discussed for ^{13}C in ref. [8], where a parity doublet for the linear chain states has been identified. The predicted chain states in the carbon isotopes can be considered as the first case of nuclear states with hyperdeformation with an axis ratio of 3 : 1.

There have been very succesful theoretical descriptions of the dimer states based on the method of Antisymmetrised Molecular Dynamics (AMD) [32] by Horiuchi and Kanada-En'yo *et al.* [33–38]. The results gave strong support for the molecular structures in $^{9-12}$Be. The same method has also been applied to the C isotopes [13,39–41].

More recent work based on the explicit use of molecular configurations, has been applied by Itagaki *et al.* to Be isotopes [42,43] and to C isotopes, in particular for $^{14-16}$C [3,5,14]. Using the molecular orbital concept for the prolate states, the presence of a third centre in the linear arrangement will introduce in first order, as in physical chemistry, one more basis state (see ref. [8]). In order to form the covalent states in a linear ^{14}C molecule, the two valence neutrons have to be placed into basis states at the three centres, resulting in a splitting in the number of states. The basis states can be described with Hückel wave functions as in atomic molecules, and the lowest state is expected just below the $3\alpha + x$n threshold [1,6,8].

An important aspect, however, will enter in the case of *nuclear molecules* with two valence neutrons, because of a strong short-range pairing interaction. This is well observed in the ^{10}Be ground state with a two-neutron binding energy of 8.8 MeV. For the case of ^{14}C this will lead to the occurrence of intrinsically reflection-asymmetric chain states [12,44], based on the ^{10}Be+α structures. This structure will give rise to parity doublets, where two nucleons remain concentrated just between two of the three α-particles. Thus, the discussion of the ^{14}C chain states will either be based on the basic covalent molecular structures (chain states) identified in ref. [8] for ^{13}C, or on the subdivision into the substructures like ^{10}Be and α. These configurations are schematically shown in fig. 3. In the fully symmetric configurations calculated by Itagaki [3] the bending modes of the 3α-particle chains are expected to be stabilised by the extra neutrons in the covalently binding molecular configurations (this happens only in the mixed, $\pi \otimes \sigma$ configurations).

In addition *oblate cluster states* are expected in ^{14}C. They will be connected to the crossing of orbits on the left (oblate) side of the diagram in fig. 1, namely for the deformed shell with $N = 6$ for ^{12}C. The second 0^+ state of ^{12}C has long been considered as a 3α-cluster state; however, no specific orientation of the three alphas can be defined and the bending mode is expected to be an important part of the wave function [45]. This state must be described as a weak-coupling state with an oblate ^{8}Be+α configuration [46], which is also described in recent work as an α-condensate [7]. The oblate cluster states of ^{14}C can have overlap (and mix) with shell model states based on the $^{12}\text{C}_{\text{g.s.}}$, or on the excited state giving a $(2^+) \otimes (2\text{n})_{nlj}$ configuration, while the prolate shapes are expected *not* to be mixed with such shell model states. These considerations will be reflected in the selectivity for the population

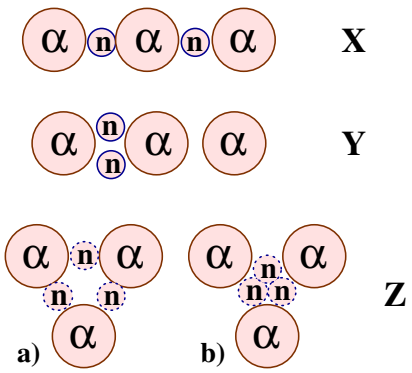

Fig. 3. Schematic illustration of the triangular configurations and of the two possible linear-chain configurations in ^{14}C with different sharing of the two neutrons. X: this configuration is the most symmetric one and has positive parity; Y: is intrinsically reflection asymmetric, with parity doublets; Z: oblate shapes, a) with a node of the valence particles wave function at the centre, due to the triangular shape it has spin parity $J^\pi = 3^-$ (the indicated three neutrons shall symbolize the two valence neutrons delocalised along the three α-particles); b) with the maximum of the valence particles wave function at the centre, with $J^\pi = 0^+$.

of ^{14}C states in different reactions with 2n-transfer in comparison with the "^{5}He" transfer, (^{7}Li, d), and other reactions discussed in the next section.

To summarise, *three different cluster configurations* can be expected in ^{14}C:

i) *linear reflection-symmetric* chains corresponding to the (α-n-α-n-α) configuration with the valence particles equally distributed among the three basis centres, the "X-configuration" in fig. 3. The valence particles density distributions will be concentrated outside the symmetry axis (see ref. [8]) for the π-bonds; for the σ-bonds the neutrons should be concentrated on the axis. Mixed π-σ configurations can also be considered [3].

ii) *linear* intrinsically *reflection-asymmetric* configurations corresponding to the structure α-2n-α-α with the two valence neutrons in the same covalent π-bond as in the case of ^{10}Be(g.s.) (with pairing energy). This is the Y-configuration in fig. 3, giving rise to parity inversion doublets.

iii) *oblate* configurations related to a *triangular structure*, with σ-bonds between two α-particles. As discussed in refs. [5,8], the π-bonds would penetrate the α-particles and should be hindered by the Pauli principle in this configuration.

The linear "X" and "Y" configurations of ^{14}C represent cases with very different binding energy, because the two neutrons are very strongly bound in ^{10}Be due to the residual pairing interaction. The band head for the "Y"-configuration is expected close to the threshold for ^{10}Be + α at 12.012 MeV, and thus well below the other threshold (20.4 MeV) for the "unbound chain" with the structure (α-n-α-n-α). Because of the intrinsic reflection asymmetry of the Y-configuration, the related deformed bands must appear as parity inversion doublets (see refs. [11,12]) with quantum numbers $K = 0^+$ and $K = 0^-$ for ^{14}C. The states would be associated with symmetric and antisymmetric wave functions constructed from the combination of the two possible ways to share the 2n-covalent bond in the "Y"-configuration (see fig. 13 below). The positive-parity members would be the lowest in excitation energy. The splitting of the two bands will be proportional to the non-orthogonality term Δ; this is the probability to transfer the two neutrons between the two configurations, as indicated in fig. 13. The symmetric "X"-configuration should exist at an excitation energy below the decay threshold of 20.40 MeV into the $3\alpha + 2$n channel. Its energy will be determined by the covalent binding effect of the π-orbitals for the two valence nucleons, approximately 2×1.66 MeV, with an additional small effect due to the residual pairing interaction in the very extended density distribution. Therefore the band head is still expected at a higher excitation energy than the other configuration.

Itagaki *et al.* [3–5] have recently performed calculations for the symmetric linear chains and for the oblate (triangular) shapes. They obtain energies for the triangular shapes also below the threshold for ^{10}Be + α (12.012 MeV). These oblate cluster states, which appear well below this threshold, should show mixing with other deformed shell model configurations related to the oblate ground state of ^{12}C as mentioned before.

In order to identify the mentioned cluster states in ^{14}C we proceed as in the case of ^{13}C [8,9] by trying to achieve a *complete spectroscopy*. We identify first in ^{14}C the single-particle configurations with two neutrons. We investigate the structure of the remaining states populated in multi-nucleon transfer reactions, where multi-particle multi-hole configurations (involving in particular also proton excitations) become dominant. These potentially deformed states are then identified and we can predict a number of rotational bands connected to large deformations. Some of these states, if related to clustering, will have intrinsically reflection-asymmetric shapes and should be grouped into bands as parity doublets with band heads below the energies of the relevant thresholds.

From these data we will derive moments of inertia. In order to compare these moments of inertia, θ, with values of other light systems. We will use the simple parametrisation for the excitation energies of the rotational bands, with the parameters θ and E_0:

$$E(J) = \frac{\hbar^2}{2\theta}[J(J+1)] + E_0. \quad (1)$$

The Coriolis coupling may actually change the expression for the moments of inertia, but for the purpose of this approach it will be sufficient. The intrinsic structure of the molecular orbital configurations based on the deformed shell model or the cluster model, as already used for ^{13}C chain states [8], will be described in an independent paper [19].

From a simple *shell model* point of view the lowest excited positive-parity states of $A = 14$ nuclei consist of two valence particles in the *p*-shell or the *sd*-shell. A number of shell model calculations have been performed starting from ^{12}C described as a closed $(1s_{1/2})^4(p_{3/2})^8$ core to which one particle in the $p_{1/2}$-shell and one in the *sd*-shell are coupled, giving a well-defined number of states. For the higher excited states of ^{14}C we expect many states with multi-particle multi-hole excitations, with valence particles in the *sd*- and *f*-shells for neutrons.

The ^{14}C nucleus has two well-defined holes in the $p_{1/2}$-shell. Proton excitations with holes in the $p_{3/2}$-shell will appear at higher excitation energy, the latter will particularly be related to cluster states, as will be shown later.

The lowest negative-parity states in ^{14}C can be described by exciting one neutron from the $p_{1/2}$- or $p_{3/2}$-shell to the *sd*-shell, leaving three holes in the *p*-shell. There are also possible mixed neutron/proton excitations appearing as (1p-3h) or (2p-4h) for positive- and (3p-5h) for negative-parity states, which are again related to cluster states. For these states the ^{12}C core excited into the 2^+ state at 4.44 MeV (which can be a proton or neutron excitation) can be used to build "core-excited states". For some of these states we can also assume that a valence particle is coupled to the lowest negative-parity state in ^{12}C (like to the 3^- state of particle-hole character).

3 Recent experimental results for ^{14}C

3.1 Results for 2-neutron and 2-proton transfer

We have studied three different types of reactions, the 2n-stripping to ^{12}C, the 2p pick-up from ^{16}O and the ^{5}He transfer to ^{9}Be. The different two-nucleon transfer reactions have been measured using the Q3D magnetic spectrometer at the ISL accelerator facility at the HMI Berlin. The reactions are the $(^{14}\mathrm{N}, ^{12}\mathrm{N})$, $(^{15}\mathrm{N}, ^{13}\mathrm{N})$ and $(^{16}\mathrm{O}, ^{14}\mathrm{O})$ on ^{12}C, as well as the $^{16}\mathrm{O}(^{15}\mathrm{N}, ^{17}\mathrm{F})^{14}\mathrm{C}$ pick-up reaction.

Details of the experimental set-up have been described previously [27]. We have chosen several projectiles: ^{14}N, ^{15}N and ^{16}O, in order to have different selectivity. The ejectiles have no excited states which are stable to particle decay; their energy spectra thus represent the excitation energy spectrum of ^{14}C. The beam energies $E_{\mathrm{lab}} = 216, 241$ and 233 MeV, respectively, correspond to ≈ 15 MeV/nucleon. The transferred angular momentum is $\approx 2.3\hbar$ per nucleon. In the stripping process we are thus populating the $p_{1/2}$-shell, but dominantly the $d_{5/2}$- and $d_{3/2}$-shells, with a good probability to reach the $f_{7/2}$-shell. The *s*-shell configurations are only very weakly populated, due to dynamical mismatch for the low angular-momentum transfer, as illustrated quantitatively in ref. [25]. We mention some other dynamical facts about the reaction, which are important in our study. At the intermediate energies an important feature is the selectivity in the population in single-particle orbits of different spin couplings. At very high relative velocities [47,48] the initial configuration (orientation) of the spin of the single nucleon becomes important for the population of the final states. A special selection rule appears: transitions between the two nuclei are strongly enhanced if the spin-orbit coupling $\mathbf{j}_x = [\mathbf{l} + \mathbf{s}]$ is the same, namely for $j_>$ to $j_>$, or $j_<$ to $j_<$. Transitions from $j_>$ to $j_<$ become weaker. However, the differential cross-section is proportional to the angular-momentum transfer and to the final spin value; these effects are important for two-nucleon transfer and at very negative *Q*-values, like in our case.

For our reactions the following single-particle configurations have to be considered: in the $(^{16}\mathrm{O}, ^{14}\mathrm{O})$ reaction two neutrons in the $p_{1/2}$-shell are involved coupled to total spin zero; the same holds for the $(^{15}\mathrm{N}, ^{13}\mathrm{N})$ reaction, but for the $(^{14}\mathrm{N}, ^{12}\mathrm{N})$ reaction we may expect a different selectivity, because a $p_{1/2}$ and a $p_{3/2}$ particle are involved and they are coupled to spin one. The influence of these is observed for example by the larger population of the unnatural-parity states at 16.43 MeV (4^-) and 14.00 MeV (3^+) and in particular for the high-lying 2^+ states, which are only well observed in the $(^{14}\mathrm{N}, ^{12}\mathrm{N})$ reaction.

The strongly populated states observed in the two-neutron stripping reaction (spectra are shown in fig. 4) must be dominantly connected to *stretched* two-neutron configurations, combinations of two orbits coupled to a maximum spin due to the rather negative *Q*-values. Different combinations are possible for the two neutrons stripped into the following configurations, and their population will be different:
a) $s_{1/2}$, expected to be weak,
b) $p_{1/2}$, $d_{3/2}$ expected to be medium,
c) $d_{5/2}$, expected to be strong,
d) eventually combinations of these with $f_{7/2}$-orbitals at the higher excitation energies, these should also be strong. As stated we expect a weak population of states with configurations consisting of combinations with the 2*s*-orbital. The states with different combinations of the *p*- and *f*-orbitals are expected to be seen; however, the strongest transitions must be observed with two neutrons in the *d*-orbitals.

For the stretched configurations we can use the simple shell model approach of Tsan Ung Chan [49,50] discussed in sect. 4.2 and obtain predictions for the excitation energy of the two-nucleon high-spin states. The excitation energy is calculated as the sum of the two individual single-particle energies (also for hole states) plus a pairing energy, if the two nucleons are identical. The energy position of stretched configurations for the mirror nucleus ^{14}O obtained by Kraus *et al.* [48], can be used for comparison; in this work a good agreement is observed between experiment and theoretical considerations based on the model mentioned. In this approach excitation energies can be predicted also for ^{14}C by using eq. (2) and the experimentally observed energies of the known single-particle neutron orbitals in ^{13}C (see table 4 in sect. 4.2).

For the spectra from 2n-stripping experiments shown in fig. 4, the measured energy positions of the states (and some of the predicted energies with eq. (2)) are compiled in table 1. We see many high-lying states in ^{14}C populated in

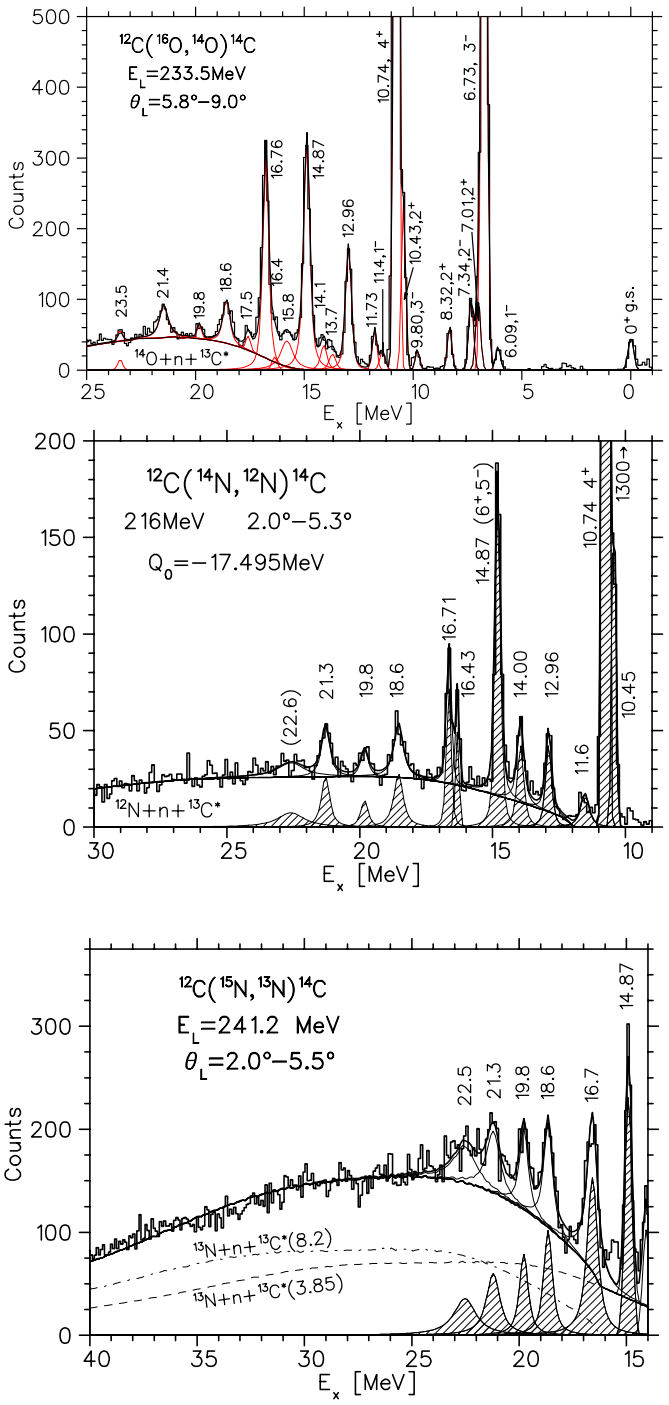

Fig. 4. Spectra for 2n-transfer reactions on ^{12}C, obtained with the Q3D spectrometer at the ISL accelerator facility, with three different projectiles ^{16}O, ^{14}N, and ^{15}N, respectively at an incident energy of approximately 15 MeV/nucleon. The angular range of the Q3D opening is indicated. The magnetic-field settings for the two lower spectra have been chosen to emphasize the higher–excitation-energy region.

the 2n-transfer reactions (sometimes not resolved) which are also populated in the high-resolution ^{9}Be(^{7}Li, d)^{14}C reaction shown in fig. 9 below. However, for many of these states *no analog states are observed* in the 2p-stripping reaction leading to the mirror nucleus ^{14}O shown in fig. 5. We believe that these "new" states at higher excitation energies in ^{14}C are the candidates for strongly clustered molecular states, because the Coulomb interaction would make them usually unbound in ^{14}O for the case of two valence protons.

Table 1. Two-neutron states in ^{14}C predicted and *observed in 2n-transfer reactions*. The predictions are based on the ground-state configuration of ^{12}C (or the 2^+ state, see text) and eq. (2) using the values of the single-particle energies in table 4 below. The "–" sign indicates a non-stretched configuration, whose real energy is expected to be higher in excitation energy. The other indications are as follows: no: not observed in the present 2n-transfer, but known from other work; w: weakly observed; s: strong (or very strong, vs) transitions. Some predicted configurations are not observed because they are weakly populated for dynamical reasons (*e.g.*, for $l = 0$ the cross-section is reduced because of the unfavorable dynamical matching conditions [25]). The spin values without parentheses are from [51]. The proton excitation indicated as $\pi(2^+)$ for the ^{12}C$^*_{2^+}$ is introduced as a supplementary configuration. Multiple configuration entries for the same state suggest configuration mixing.

J^π	Neutron conf. (^{12}C) $\otimes$ (nlj) $\otimes$ (nlj)	E_x (MeV) eq. (2)	E_x (MeV) this work	2n trans.
0^+	(g.s.) $\otimes$ $(p_{1/2})^2$	0.0	0.0	
1^-	(g.s.) $\otimes$ $p_{1/2}$ $\otimes$ $s_{1/2}$	6.32	6.09	w
0^+	(g.s.) $\otimes$ $(sd)^2$		6.59	no
3^-	(g.s.) $\otimes$ $p_{1/2}$ $\otimes$ $d_{5/2}$	7.08	6.73	vs
0^-	(g.s.) $\otimes$ $p_{1/2}$ $\otimes$ $s_{1/2}$	6.32–	6.9	no
2^-	(g.s.) $\otimes$ $p_{1/2}$ $\otimes$ $d_{5/2}$	7.08–	7.34	w
2^+	$\pi(2^+)$ $\otimes$ $(psd)^2$		8.32	w
2^+	(g.s.) $\otimes$ $s_{1/2}$ $\otimes$ $d_{5/2}$	10.17	8.32	w
0^+	(g.s.) $\otimes$ $(sd)^2$		9.74	no
3^-	$\pi(2^+)$ $\otimes$ $p_{1/2}$ $\otimes$ $s_{1/2}$	10.76	9.80	w
2^+	$\pi(2^+)$ $\otimes$ $(psd)^2$		10.43	w
2^+	(g.s.) $\otimes$ $s_{1/2}$ $\otimes$ $d_{5/2}$	10.17	10.43	w
4^+	(g.s.) $\otimes$ $d_{5/2}$ $\otimes$ $d_{5/2}$	10.93	10.74	vs
1^-	$\pi(2^+)$ $\otimes$ $p_{1/2}$ $\otimes$ $s_{1/2}$	10.76–	11.40	no
1^-	$p_{1/2}$ $\otimes$ $d_{3/2}$	11.43	11.40	no
4^-	$\pi(2^+)$ $\otimes$ $p_{1/2}$ $\otimes$ $d_{5/2}$	11.52–	11.66	no
4^+	(g.s.) $\otimes$ $p_{1/2}$ $\otimes$ $f_{7/2}$	13.98	11.73(3)	w
3^-	$\pi(2^+)$ $\otimes$ $p_{1/2}$ $\otimes$ $d_{5/2}$	11.52–	12.96(4)	s
			13.7(1)	w
(3^+)	(g.s.) $\otimes$ $p_{1/2}$ $\otimes$ $f_{7/2}$	13.98–	14.0(1)	w
6^+	$\pi(2^+)$ $\otimes$ $d_{5/2}$ $\otimes$ $d_{5/2}$	15.37	14.67(5)	s
5^-	$\pi(2^+)$ $\otimes$ $p_{1/2}$ $\otimes$ $d_{5/2}$	11.52	14.87(4)	s
5^-	(g.s.) $\otimes$ $d_{5/2}$ $\otimes$ $f_{7/2}$	17.83–	14.87(4)	s
			15.75(8)	w
(6^+)	$\pi(2^+)$ $\otimes$ $d_{5/2}$ $\otimes$ $d_{3/2}$	19.72	16.4(1)	w
(6^-)	(g.s.) $\otimes$ $d_{5/2}$ $\otimes$ $f_{7/2}$	17.83	16.72(5)	s
	$\pi(2^+)$ $\otimes$ $d_{5/2}$ $\otimes$ $p_{1/2}$	11.52	16.72(5)	w
			17.5(1)	w
			18.6(1)	w
(2^+)	(g.s.) $\otimes$ $d_{3/2}$ $\otimes$ $d_{3/2}$	19.63	19.8(1)	w
			21.4(2)	w
			22.5(3)	w
			23.5	w

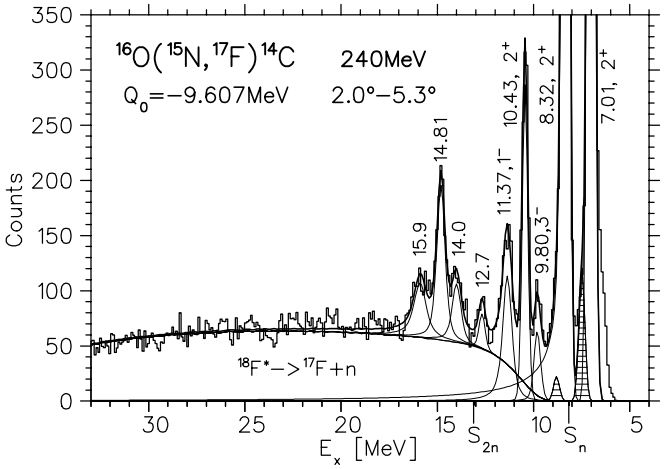

Fig. 5. Spectrum for the 2p pick-up reaction on ^{16}O, obtained with the Q3D spectrometer at ISL Berlin at an energy of 16 MeV/nucleon.

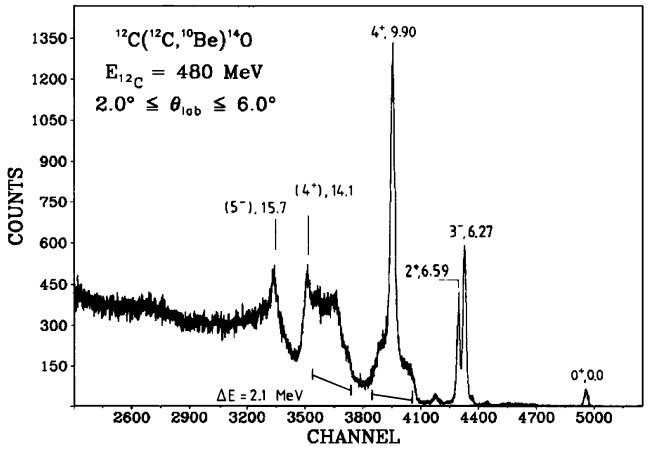

Fig. 6. Spectrum for the 2p-transfer reaction ^{12}C(^{12}C, ^{10}Be)^{14}O obtained at 480 MeV, at 40 MeV/nucleon (from ref. [48]). The bars indicate the region of the γ-recoil broadened ^{10}Be(2^+) state populated in combination with the 3^- and 4^+ states.

Table 2. States populated in ^{14}C in the 2p pick-up reaction (^{15}N, ^{17}F) on ^{16}O, at $E_{\rm lab} = 240$ MeV. The configurations predicted in ref. [52] are marked by "*". The lifetimes τ or line widths Γ are given in the last column.

J^π, E_x ref. [51]	E_x (MeV) this work	Proton conf. (nlj)	τ, or Γ (keV)
2^+, 7.01	7.01	$p^{-1}_{3/2}p^{-1}_{1/2} \otimes \nu(psd)^2$,*	0.0
2^+, 8.317	8.32	$p^{-1}_{3/2}p^{-1}_{1/2} \otimes \nu(psd)^2$,*	1.55 fs
3^-, 9.801	9.80	$p^{-2}_{3/2}p^{-1}_{1/2}s^1_{1/2}$	12.4 ps
2^+, 10.425	10.43	$p^{-1}_{3/2}p^{-1}_{1/2} \otimes \nu(psd)^2$,*	< 50 keV
1^+, 11.306	11.37	$p^{-1}_{3/2}p^{-1}_{1/2}$,*	350
1^-, 11.395	11.37	$p^{-2}_{3/2}p^{-1}_{1/2}s^1_{1/2}$	50
	12.7(1)		300
2^+	14.0(1)	$p^{-2}_{3/2}$,*	250
	14.81(7)		250
	15.9(1)		600

The weaker lines at higher excitation energy observed in the 2n-transfer are expected to be related to core excitations ($^{12}C^*_{2^+}$ and $^{12}C^*_{3^-}$), or to the population of the $d_{3/2}$- and $f_{7/2}$-shells. In the first case structures with multiparticle multi-hole excitations which lead to structures like $(p_{3/2})^{-1} \otimes p_{1/2} \otimes (sd)^2$ are expected, which can be mixed with other configurations. The states built on a core excitation (2^+) would be populated in a two-step process with a collective excitation as a first step, a process well established in two-nucleon transfer [53]. The states would attain a smaller decay width, because of the increased energy for the particle thresholds and larger spins as described in the weak-coupling model.

In addition we show in fig. 5 our data on the 2p pick-up from the reaction ^{16}O(^{15}N, ^{17}F)^{14}C at 240 MeV. The observed states are compiled in table 2, we see that the 2p pick-up reaction excites very different states as compared to the 2n-stripping reaction, actually only lower-spin values are expected to be populated in the former. However, some strongly excited states seen in the cluster transfer (^{7}Li, d) reaction (and others cited later) also appear here, pointing to the particle-hole structure of the cluster states in ^{14}C populated in the latter reaction. The higher-lying states in ^{14}C, which are excited in 2n-stripping, are not seen in the 2p pick-up reaction; they may involve the collective particle-hole (1p-1h) structure of the 2^+ state with additional *neutrons* in the (sd)-shell. In the present pick-up reaction these can only be obtained from the (4p-4h) correlations of the ground state of ^{16}O. The 4p-4h admixtures involve nucleons in the *sd*-shell, and in this way also negative-parity states can be populated in 2p pick-up.

Almost all states in table 2 are rather weakly populated or not seen in the other reactions, like the 2n-transfer shown in fig. 4; some states (like the state at 15.9 MeV) are not observed in the other reactions (fig. 4 and figs. 8, 7 and 9 below). The states listed in table 2, however, have limited information due to the limited resolution of this experiment, where it was not possible to clearly separate and identify all relevant levels. There is a strong correspondence to the hole states recently obtained in a large-scale shell model calculation [52]. Some relation to states, which are also populated in the high-resolution spectrum of the ^{9}Be(^{7}Li, d)^{14}C reaction, can be established. More discussions will be given in sect. 4.

In the study of the 2p-stripping on ^{12}C at 480 MeV in the ^{12}C(^{12}C, ^{10}Be)^{14}O reaction [48], a pronounced population of states in ^{14}O has been observed (fig. 6) and from the mentioned considerations some assignments of configurations have been proposed.

The states observed in ^{14}O are the isospin analogs of states in ^{14}C; strong transitions to stretched configurations are observed in our case for the $(d_{5/2} \otimes p_{1/2})_{3^-}$ state at 6.73 MeV (6.27 MeV in ^{14}O), for the $(d_{5/2})^2_{4^+}$

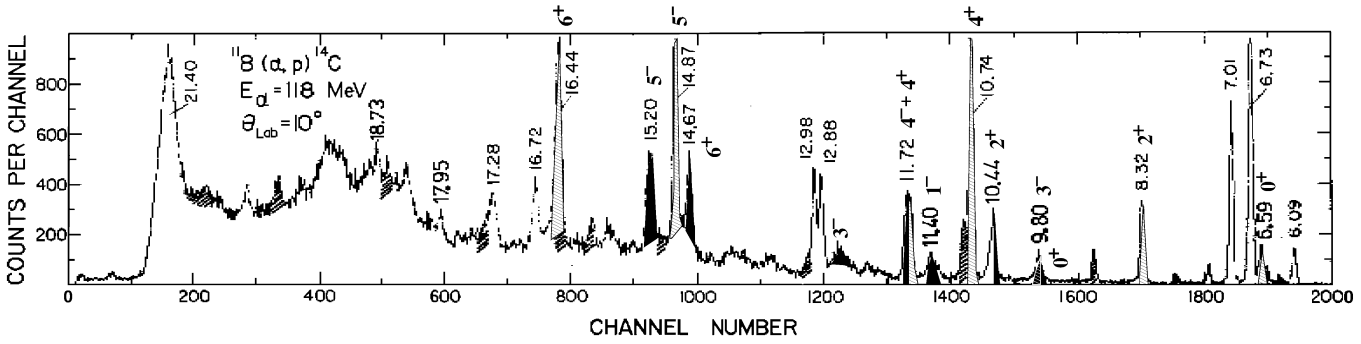

Fig. 7. Spectrum for the triton transfer reaction ^{11}B(α, p) (adopted from ref. [54]); compare also to fig. 8. The proposed band structure is indicated by black for prolate and by shaded (inclined \\) for oblate bands with $K = 3^-$ and $K = 0^-$. Shading (inclined //) is also used to indicate contaminant lines.

state at 10.74 MeV (9.9 MeV in ^{14}O), for a state at 14.87 MeV (14.1 MeV in ^{14}O), which is assigned as 4^+ in ref. [48]; see, however, our discussion of this assignment in the next section. Further the strong peak observed at 16.72 MeV in ^{14}C is expected to be the highest spin of the $(d_{5/2} \otimes f_{7/2})_{6^-}$ configuration (see table 1), and corresponds to the 15.7 MeV state observed in ^{14}O. The analog of the 12.96 MeV (3^-) state seen in the spectrum in ^{14}C (fig. 4) expected around 12.5 MeV in the case of ^{14}O is most likely covered by the gamma-recoil structure in fig. 6, due to the decay of the 2^+ state at 3.368 MeV in ^{10}Be (combined with the 9.60 MeV state) creating the strong shoulder at the excitation energy of 12.5 MeV in ^{14}O.

3.2 Results for other multi-nucleon transfer reactions

A very useful reaction for our study is the triton transfer reaction, which has been studied with good resolution via the ^{11}B(^{6}Li, ^{3}He)^{14}C [55] and the ^{11}B(α, p)^{14}C [54] reactions. These reactions show a remarkable selectivity to "oblate" cluster states, because ^{11}B represents a $p_{3/2}$-hole in the oblate ^{12}C nucleus. Due to the large negative Q-value in the region of high (10–18 MeV) excitation energy in ^{14}C (the ground-state Q-values are +4.803 MeV and +0.784 MeV, respectively), these two reactions also show a marked selectivity to high-spin states.

We reproduce in figs. 7 and 8 the spectra from refs. [54] and [55]. The spectra show a very small background, also because the boron targets can be obtained free of oxygen and carbon contaminants. Remarkable is a gap between the states at 12.96 MeV and 14.67 MeV, also observed in the (^{7}Li, d) reaction (where it is partially covered by contaminants, see below). There may be some broad states in this region; however, we observe, at 14.0 MeV a state in proton pick-up and in the (^{14}N, ^{12}N) reaction, the latter being an indication for unnatural parity like 3^+ or 2^-. Such states are not expected to be strongly populated in cluster transfer reactions. The two spectra show as the strongest peaks those states, which are later assigned to the $K = 0^+$ oblate rotational band (see also fig. 12 below). Similarly the oblate $K = 3^-$ band is well observed, whereas the proposed prolate states are rather weak, consistent with our interpretation, that the parantage between target configuration and final state determines the probability of the reactions (see discussion in the next section).

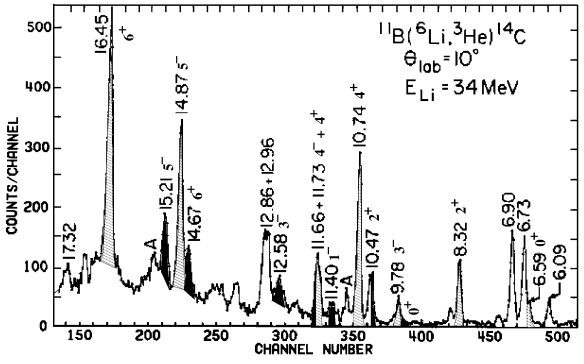

Fig. 8. Spectra for the triton transfer reaction on ^{11}B (adopted from ref. [55]) showing strong selectivity to oblate states. The proposed band structure is indicated by black for prolate and shaded for oblate bands ($K = 3^-$ and $K = 0^-$).

3.3 Results for the reaction ^{9}Be(^{7}Li, d)^{14}C

A spectrum of the ^{5}He transfer reaction ^{9}Be(^{7}Li, d)^{14}C has been measured with the Q3D spectrometer at the accelerator laboratory of the LMU and TU Universities in München at an energy of 44 MeV. The target thickness of 60 μg/cm^2 has been chosen to have an overall resolution of 40–50 keV. The reaction angle has been set to $\theta_{\rm lab} = 10°$, with a total horizontal opening angle of 6.0°. Since the spectrometer range in the focal plane is approximately 17% in energy, the spectrum has been obtained using 6 overlapping magnetic-field settings. We were able to observe states in ^{14}C up to 21.4 MeV. Although the ^{9}Be

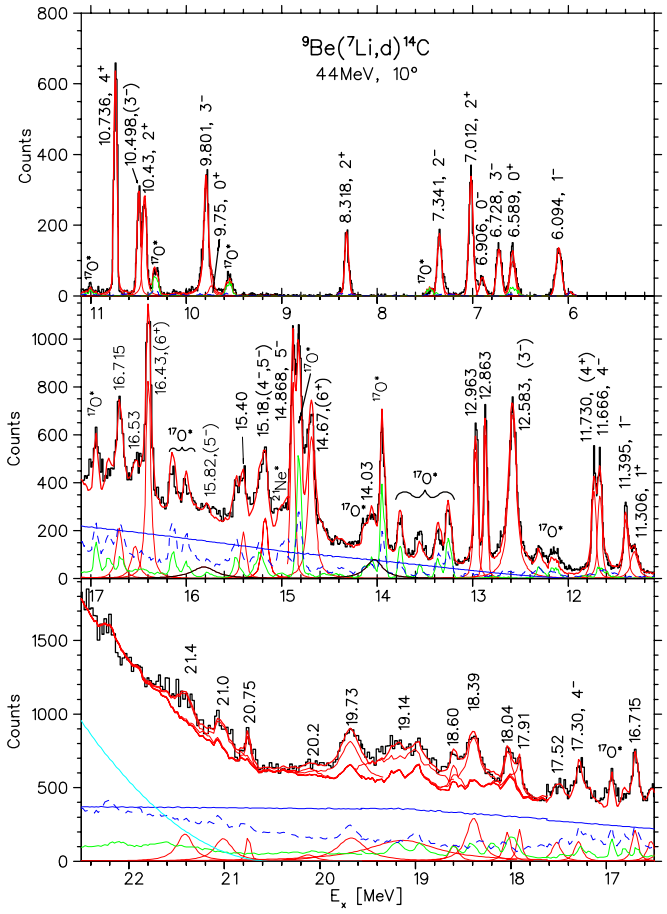

Fig. 9. Deuterium spectrum from ^{5}He transfer on ^{9}Be obtained with a ^{7}Li beam of $E_{\rm lab}$ = 44 MeV (approximately 6.3 MeV/nucleon) at the Q3D spectrometer of the Accelerator Laboratory in Munich. The structured backgrounds shown are 3- and 4-body continua, or have been measured with ^{12}C and ^{16}O targets (full and dashed lines, respectively), indicated as ^{17}O* for ^{12}C and ^{21}Ne* for ^{16}O.

target is rather pure, we have measured for the whole range also background spectra for the ^{12}C and ^{16}O contaminants, respectively, with the same magnetic-field settings and with unchanged multipoles. This results in kinematically non-focused structures, which are used unchanged in the final fit to the spectrum shown in fig. 9. The contaminant lines due to ^{12}C and ^{16}O (from carbon build-up and a small oxidation of the target) are marked as ^{17}O* and ^{21}Ne*, respectively.

For the reaction mechanism we expect a dominant contribution from the sequential transfer of an α-particle and a neutron (or vice versa). This particular reaction on ^{9}Be may not be very selective, because with the alpha-particle transfer, both oblate states and prolate cluster states can be populated, the extra neutron being free to populate the $p_{3/2}$-, the $p_{1/2}$-, the $s_{1/2}$-, as well as the $d_{5/2}$- and $d_{3/2}$-shells. In a CRC calculation to be performed in the future for this reaction, both sequences have to be included; in the sequence where the neutron transfer occurs first a larger variety of intermediate excited states in ^{10}Be has to be considered. This points to the expectation that with a ^{10}Be target in the ^{10}Be(^{7}Li, t)^{14}C reaction a different selectivity is expected. This effect of different selectivity on ^{9}Be and ^{10}Be targets has been observed before (refs. [25], and [28]).

The spectrum shown in fig. 9 is similar to the spectrum observed in the ^{9}Be(^{6}Li, p) reaction in ref. [56] obtained at a much lower energy, $E_{\rm lab}$ = 17 MeV; at this energy the compound nuclear process is dominating. In our case there is a different selectivity, due to direct transfer processes, but there is also the preference for high-spin states due to the large angular-momentum mismatch between the mass-7 projectile and the ejectile of mass 2.

With this high-resolution spectrum (fig. 9) and using the results of the other spectra discussed before (figs. 4, 5, 7 and 8) we are able to draw several important conclusions:

a) The reactions have very different selectivity, most states are populated in the ^{9}Be(^{7}Li, d) reaction.

b) The stretched single-particle configurations of high spin, that are strongly populated in the 2n-stripping reaction, are also strong in the spectrum of the ^{9}Be(^{7}Li, d) reaction (and in the triton transfer), mainly because of their large spin values.

c) Some strong peaks in the 2n-transfer spectra are due to overlapping states, not separated in energy, but separated in the ^{9}Be(^{7}Li, d) reaction.

d) Many *narrow* states are observed at higher excitation energy in the ^{9}Be(^{7}Li, d) reaction well above the particle emission thresholds for simple decays, like for ^{13}C + n (8.176 MeV) or for ^{10}Be + α (12.012 MeV).

e) As already noted, the weaker lines in the 2n-transfer, which may be related to core excitations, are well observed in the (^{7}Li, d) reaction. The strongest transitions are expected to proceed via the ^{12}C(2$^+$) state. Their configurations are obtained with holes (protons, π; or neutrons ν) in the $p_{3/2}$-shell, namely configurations like $(p_{3/2})^{-1} \otimes d_{5/2}$ and other higher shells. These can also be easily populated by neutron plus alpha-particle transfer on ^{9}Be.

f) The 2p pick-up reaction from ^{16}O shows very strong peaks due to the removal of protons from the $p_{1/2}$- and in particular from the $p_{3/2}$-shell. These states are very weak or not seen at all in the 2n-stripping reaction. Some of these 2p transitions are also seen in the ^{9}Be(^{7}Li, d) reaction, indicating a common structure with multi-hole multi-particle configurations. However, the pick-up reaction cannot populate configurations with neutrons in the $d_{3/2}$- and $f_{7/2}$-shells, in fact no states are populated beyond 16 MeV excitation energy. We can use this observation in the interpretation of the structure of high-lying states.

Many states populated in the 2n-transfer reactions are also expected to appear in the ^{5}He transfer. The differential cross-section will thus predominantly depend on the angular-momentum transfer of the neutron and of the α-particle, and as usual on the spin multiplicity of the final states, given by $(2J + 1)$. In order to classify the states their relative strength is compared in table 3 after

Table 3. Excitation energies (E_x) of states in ^{14}C *observed in the* (^{7}Li, d) *reaction*. The proposed spins and parities are given in the first column. The assignments without parentheses are from ref. [51]. In column 3 the configurations and parities (Conf/(Par)) are given, used to interpret the rotational bands of the deformed states, these are marked as oblate or prolate, or the configurations are given explicitly. We have marked with "ex" the extra states not used in the compilation for rotational bands. Relative yields (divided by $2J+1$) are given in column 4, they are normalized to the 2^+ state at 7.012 MeV, which has a value of 200. For the states with unassigned spins, the values are normalized with a spin value of 2, sometimes indicated as (2^+). Additionally, for comparison, the population strength *observed in the 2n-transfer* is indicated in this column by a character using the following code: (+) - strong in 2n; (*) - average or weak in 2n; (−) - not seen in 2n. The lifetimes τ or line widths Γ are given in the last column.

J^π	E_x (MeV) this work	Conf/(Par) proposed	$N/(2J+1)$ relative	τ, or Γ (keV)
0^+	0.0	mixed		0.0
1^-	6.09	$p_{1/2}s_{1/2}$	$179^{(*)}$	< 7 fs
0^+	6.59	obl (+)	$338^{(*)}$	3 ps
3^-	6.73	$p_{1/2}d_{5/2}$	$65^{(+)}$	66 ps
0^-	6.906	$p_{1/2}s_{1/2}$	$180^{(-)}$	25 ps
2^+	7.012	$\pi p_{3/2}^{-1}p_{1/2}^{-1}$	$\mathbf{200}^{(-)}$	9 fs
2^-	7.348	$p_{1/2}d_{5/2}$	$101^{(*)}$	111 fs
2^+	8.318	obl (+)	$97^{(+)}$	3.4
0^+	9.74	prol (+)	$50^{(*)}$	–
3^-	9.80	obl (−)	$183^{(*)}$	45
2^+	10.43	prol (+)	$263^{(+)}$	25
(3^-)	10.498	ex	$131^{(-)}$	12
4^+	10.736	obl (+)	$158^{(+)}$	10
1^+	11.306	ex	$174^{(+)}$	40
1^-	11.39	prol (−)	$220^{(*)}$	25
4^-	11.66	obl (−)	$95^{(-)}$	20
4^+	11.73	prol (+)	$100^{(*)}$	30
(3^-)	12.58	prol (−)	$470^{(-)}$	two peaks
	12.86	ex	$163^{(+)}$	25
	12.96	ex	$126^{(-)}$	25
	14.03	ex	(*)	100
6^+	14.67	prol (+)	$185^{(-)}$	
5^-	14.87	obl (−)	$158^{(+)}$	two peaks
(5^-)	15.18	prol (−)	$80^{(-)}$	50
(2^+)	15.40	ex	$116^{(-)}$	40
6^+	16.43	obl (+)	$179^{(*)}$	35
(2^+)	16.53	ex	$^{(-)}$	50
(1^+)	16.72	ex	$90^{(+)}$	60
4^-	17.30	ex	$^{(-)}$	80
(2^+)	17.52	ex	$125^{(*)}$	100
(2^+)	17.91	ex	$98^{(-)}$	50
(7^-)	18.03	prol (−)	$114^{(-)}$	70
	18.39	ex	$147^{(-)}$	170
	18.60	ex	$87^{(*)}$	100
	19.14	ex	–	900
(2^+)	19.73	$d_{3/2}d_{3/2}$	$491^{(*)}$	250
	20.02	ex	–	200
	20.75	ex	–	40
	21.00	ex	–	220
	21.41	ex	–	550

division by $(2J+1)$. For a comparison of structural effects all yields are normalized to the value (200) of the first 2^+ state at 7.012 MeV. Note that the states, connected to the "oblate" and "prolate" bands are all equally well populated in (^{7}Li, d), with a tendency of a cut-off at the highest excitation energies, where high spins are populated.

4 Survey of states in ^{14}C

4.1 General considerations

The experimental level schemes of ^{13}C and ^{14}C are rather well determined for excitation energies up to about 10 MeV [51]. As a guide line for the complete spectroscopy we have to inspect many theoretical approaches published for ^{14}C. Early shell model calculations [57–61] successfully describe some of the ^{14}C states up to $E_x \approx 10$ MeV. Above this energy the spectroscopic data is rather scarce so it is hard to estimate how good these models are for higher excitations.

Positive-parity states of ^{14}C were calculated by rearrangements within the $1p$-shell by Cohen and Kurath [58]. From a simple shell model view point, the ^{12}C nucleus has an almost closed $(1p_{3/2})$-shell, with a 71% $(p_{3/2})$ and 27% $(p_{1/2})$ configuration occupation.

The lower-lying states of ^{14}C would then result from adding two particles in the $p_{3/2}$ (due to the ground-state correlations), and the higher $1p_{1/2}$-, $2s_{1/2}$-, $1d_{5/2}$- or $1d_{3/2}$-orbitals. Since ^{12}C does not have a completely closed $1p_{3/2}$-subshell, some of the lower levels in ^{14}C also have admixtures of $1p_{3/2}$ *neutron* excitations. For example the lowest 2^+ state at 7.012 MeV has as the main configuration π-$(p_{3/2})^{-1}$ $(p_{1/2})^1$, and higher-lying states will have *neutron* configurations with excitations from the $1p_{3/2}$-shell to higher shells. In this context we mention that already in ^{13}C there are many states which are described to be mixed with core excitations [61]. Thus, another view of the structure of some states in ^{14}C is provided by coupling a single neutron to the ground and excited states of ^{13}C (through core excitation of ^{12}C). In ^{14}C the neutron excitations occur from a closed $(p_{3/2})$-shell and a closed $(p_{1/2})$-shell. These considerations are summarised in fig. 10. Core-excited states with pure configurations and high spin will again have narrow width, because the decay will be strongly hindered. Some of the cluster states of ^{14}C can also be reached by two-proton pick-up on ^{16}O, here again core excitation must be invoked for the structure of the states.

Shell model calculations within a full *psd*-basis for the $T = 1$ states of nuclei with mass 14 have been made by Jäger *et al.* [59], Lie [60] and Millener and Kurath [61]. Further states with the *sd*-shell are discussed in ref. [62]. Calculations within $(0+2)\hbar\omega$ configuration space have been performed by Wolters *et al.* [63]. Predictions for cluster chain states have been made in ref. [1], and more detailed calculations based on the molecular orbital approach were done by Itagaki *et al.* [3–5]. For the low-excitation region, there is also a cluster model calculation

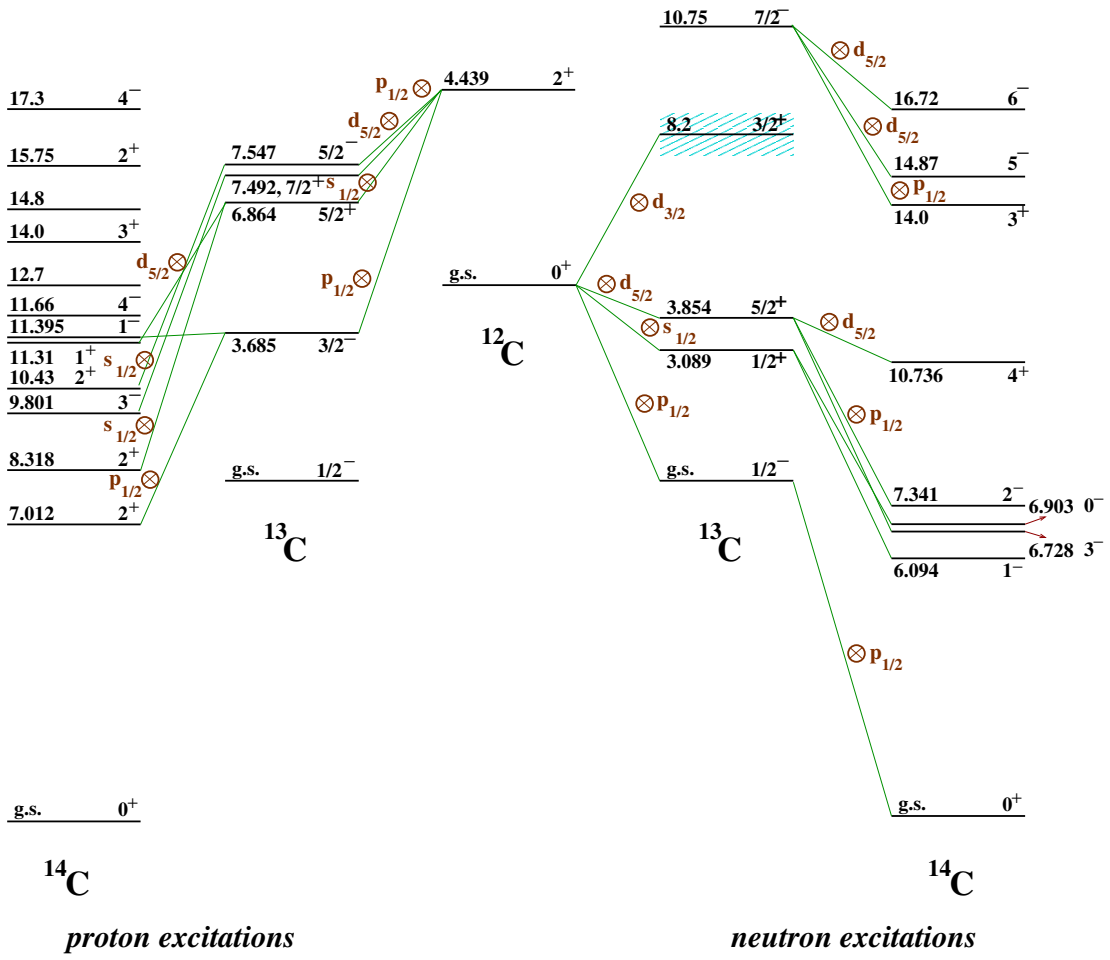

Fig. 10. Plot of energy levels of the isotopes ^{13}C and ^{14}C, which can be related to the single-particle structure in ^{13}C, or to core-excited states with the 2^+_1 state in ^{12}C. The excitation energies are shown relative to the energy of the $^{12}\mathrm{C}+xn$ threshold. On the left side of the ^{12}C spectrum we give the states of $^{13-14}$C corresponding predominantly to proton excitations, while on the right side states connected to neutron excitations are given. Most states of ^{14}C based on single-particle configurations may mix with the oblate cluster states like the second 0^+ state, which are not shown here, but see fig. 11 and sect. 3.3.

by Dufour and Descouvemont [64] using the generator coordinate method to investigate some $1p$-shell nuclei.

We proceed with the discussion of the two-neutron states, which, however, being based on the low-lying states of ^{12}C will be also related to core excitations and to the oblate deformed states.

4.2 Two-nucleon configurations in ^{14}C based on ^{12}C (g.s.) and the ^{12}C core excitations

For the discussion of the two-neutron states populated in 2n-transfer reactions, we can rely on the well-documented information of ref. [51], and we will use the already mentioned procedure from refs. [48–50] in order to localise the stretched two-neutron configurations with spins j_1 and j_2, coupled to the highest spin J. The energy of these states is given by

$$E^*(A_0+2N,j_1,j_2;J) = [2E_B(A_0+N;\mathrm{g.s.}) - \\ - E_B(A_0;\mathrm{g.s.}) - E_B(A_0+2N;\mathrm{g.s.})] + \\ + E^*_B(A_0+N;j_1) + E^*_B(A_0+N;j_2). \quad (2)$$

In this formula the binding energies $E^*_B(A_0+N;j)$ of the single-particle states in the j-orbit in the nuclei with the core $A_0(^{12}\mathrm{C_{g.s.}})$ plus one or two neutrons are needed. For this we use the experimentally determined energies of the single-particle states in ^{13}C, these are given in table 4. The states given there do not represent the full strength of each shell model orbit; however, the approach works quite reliably within a margin better than 500 keV for the prediction of the energies. Actually the energies tend to be predicted slightly too high. The case of the $d_{3/2}$-orbit is special because of its large width due to the n decay,

Table 4. Energies of single-particle configurations in ^{13}C used to interpret the strongly populated "stretched" states in ^{14}C observed in 2n-transfer on ^{12}C.

J^π ref. [51]	E_x (MeV)	J^π configuration (nlj)	Width τ or Γ
$1/2^-$	0.0	$p_{1/2}$	0.0
$1/2^+$	3.09	$s_{1/2}$	1.55 fs
$5/2^+$	3.85	$d_{5/2}$	12.4 ps
$3/2^+$	8.2	$d_{3/2}$	1100 keV
$7/2^-$	10.75	$f_{7/2}$	55 keV

however, the states of high spin with two neutrons in this configuration will still have a small width. Similarly there are uncertainties with the position of the $f_{7/2}$-orbit, the strength located at the first $7/2^-$ level cited in the table contains only 30% of the total strength.

With this approach we have calculated excitation energies of the stretched states in ^{14}C, (see table 1), which correspond to two neutrons added to the ^{12}C ground state. The non-stretched states are sometimes listed. Usually their positions are not known, but the information is eventually needed for the establishment of a complete spectroscopy. The pairing energy used here, expressed by the square brackets in eq. (2), is 3.23 MeV; it is calculated using the difference between $Q(^{14}\mathrm{C} \rightarrow {}^{13}\mathrm{C}{+}\mathrm{n}) = 8.177$ MeV and $Q(^{13}\mathrm{C} \rightarrow {}^{12}\mathrm{C} + \mathrm{n}) = 4.946$ MeV.

In addition we consider for the weakly populated states, the excitation of the core state $^{12}\mathrm{C}^*(2^+)$, which is coupled with neutron configurations. This core state can consist of proton and neutron excitations, and only in the latter case the Pauli principle will limit the neutron configurations to be placed in the p-shell. To predict such states we tentatively use the weak coupling model and add 4.44 MeV (see table 1) to the energy of the predicted stretched configurations with maximum spin, with spins by two units higher. Actually the width is expected to be smaller for pure configurations because of the increased decay thresholds. In this model a multiplet of states is obtained: the best example being the first-excited states with $J^\pi = 1/2^-$ up to $9/2^-$ of ^{11}C or ^{11}B, which are explained by the coupling of $p_{3/2}$-hole to the $^{12}\mathrm{C}^*(2^+)$ state. Similarly some of the low-lying single-particle states of positive and of negative parity in ^{13}C are strongly mixed with core excitations (refs. [8,10]).

4.2.1 States observed with two-neutron transfer

For the present discussion we use the information on the main excited states observed in ^{14}C in our two-neutron transfer as compiled in table 1. We list below the individual states (some of them not resolved, see, however, the $^9\mathrm{Be}(^7\mathrm{Li},\mathrm{d})$ reaction) with their population characteristics and give the relevant references of other work. The predictions using eq. (2) for configurations involving the $d_{3/2}$- and $f_{7/2}$-orbits must be taken with caution, because of the strong fragmentation of the strength. Mixing of these configurations with other states is to be expected, resulting in a lowering of the expected energy. Energies are given as observed, they agree usually within 10 keV with the published values of the compilation in ref. [51] unless noted differently.

0^+ g.s., and the 0_2^+ at 6.589 MeV
For the ^{14}C ground state, which is considered to be a closed-shell nucleus, a mixing with the *sd*-shell configurations of about 5% of the total strength was found in the analysis of the $^{14}\mathrm{C}(\mathrm{d},\mathrm{p})$ reaction [65], which is consistent with earlier estimates [60,66,67], while Fortune and Stephans propose a mixture of 12% with the *sd*-shell [68]. Small $1g_{9/2}$ and $1f_{5/2}$ pick-up strengths from the ground state of ^{14}C were also reported. However, such a wave function was shown by Rose *et al.* [67] to be not able to explain the greatly delayed Gamow-Teller β-decay between the ^{14}C and ^{14}N ground states; this is probably caused by a non-closed ^{12}C core. The second 0_2^+ state and the g.s. are often discussed as mixed states, due to the configuration mixing introduced by the pairing interaction [68,69]; these wave functions give a rather satisfactory result in a microscopic calculation [70] for the $^{12}\mathrm{C}(^6\mathrm{He},\alpha)^{14}\mathrm{C}$ 2n-transfer reaction. The third 0^+ state will appear with the prolate states, states connected to excited states of ^{10}Be are expected at even higher excitation energy.

6.094 MeV, 1^-, very weak
This state is rather weak in the $^{13}\mathrm{C}(\mathrm{d},\mathrm{p})$ [71] and $^{15}\mathrm{N}(\mathrm{d},{}^3\mathrm{He})$ [72] reactions, but since it is rather strong in the $^{14}\mathrm{C}(\mathrm{p},\mathrm{p}')$ [73], $^{14}\mathrm{C}(^3\mathrm{He},{}^3\mathrm{He}')$ [74] and $^{14}\mathrm{C}(\alpha,\alpha')$ [71] inelastic scattering, the $p_{1/2} \otimes s_{1/2}$ configuration is generally accepted. It is also rather strong in the $^{13}\mathrm{C}(^7\mathrm{Li},{}^6\mathrm{Li})$ [75] reaction which is consistent with such a configuration. In our two-neutron transfer reactions (fig. 4) this state is only weakly populated, as actually expected because of the low individual l-values involved for a $(p_{1/2}s_{1/2})$ configuration.

6.728 MeV, 3^-, very strong
This is the strongest peak in a number of spectra, like those for the reactions $^{13}\mathrm{C}(\mathrm{d},\mathrm{p})$ [71], $^{13}\mathrm{C}(^7\mathrm{Li},{}^6\mathrm{Li})$ [75] and $^{12}\mathrm{C}(^{10}\mathrm{B},{}^8\mathrm{B})$ [76]. It is also the strongest peak in many inelastic excitations, like the $^{14}\mathrm{C}(\mathrm{p},\mathrm{p}')$ [73], $^{14}\mathrm{C}(\mathrm{d},\mathrm{d}')$ [77], as well as $^{14}\mathrm{C}(^3\mathrm{He},{}^3\mathrm{He}')$ [74] and $^{14}\mathrm{C}(\alpha,\alpha')$ [71] inelastic scattering. In two-neutron transfer it is the second strongest peak in our reaction and in the $^{12}\mathrm{C}(^{12}\mathrm{C},{}^{10}\mathrm{C})$ [78] reaction. It is rather weak in the $^{15}\mathrm{N}(\mathrm{d},{}^3\mathrm{He})$ [72] reaction ($C^2S \leq 0.11$), and appears as a weak shoulder in the 2p pick-up, in agreement with its assignment as a $p_{1/2} \otimes d_{5/2}$ configuration.

6.903 MeV, 0^-, not seen
This state is not seen in the $^{14}\mathrm{C}(\alpha,\alpha')$ [71] inelastic scattering, where it could only be populated by a two-step inelastic transition, similar to other unnatural-parity states. It is observed in the $^{13}\mathrm{C}(\mathrm{d},\mathrm{p})$ [71] reaction. It is not observed, however, in the $^{14}\mathrm{C}(\mathrm{p},\mathrm{p}')$ [73] and

^{14}C(d, d′) [77] inelastic scattering; most likely because of limited resolution it was not separated from strong adjacent peaks at 6.728 and 7.012 MeV.

7.34 MeV, 2⁻
This state is rather strong in all simple reactions [71, 73,75,77] except in pick-up reactions like ^{15}N(d, ^{3}He) ($C^2S \leq 0.04$) [72]. It is well separated in our two-neutron transfer reaction, the weaker population being due to the $p_{1/2}$-orbit in the non-stretched $p_{1/2} \otimes d_{5/2}$ configuration (the stretched transition is the 6.728 MeV state). It is not seen in the triton transfer reactions.

8.32 MeV, 2⁺ weak
This is one of the few states populated in both, 2n-stripping (weak) and 2p pick-up (strong) reactions indicating core excitation; the overall behavior is consistent with the configuration of two-nucleon excitation into the *sd*-shell. It may be mixed with the 2^+ state at 10.43 MeV. It is well observed also in multi-nucleon transfer reactions.

9.80 MeV, 3⁻, weak
The state is well separated and weakly populated in the 2n-stripping reaction, again it is also seen in the 2p pick-up reaction indicating core excitation. It is also strong in the ^{13}C(p, π^+)^{14}C reaction which populates core-excited states. As in the previous case of the two 2^+ states, this core-excited state may be mixed with the strong (1p-1h) state 3^- at 6.73 MeV.

10.43 MeV, 2⁺, weak
This state is well seen in all simple reactions [71,73,75, 77], in particular in the 2p pick-up, and in reactions like ^{15}N(d, ^{3}He) [72]. It is not well separated in our two-neutron transfer reaction, the weaker population being due to the core excitation component and the $s_{1/2}$-orbit in the non-stretched $s_{1/2} \otimes d_{5/2}$ configuration.

10.736 MeV, 4⁺, very strong
The state is strongly populated in our 2n-transfer reactions, due to the $(d_{5/2})^2$ configuration. The spectroscopic factor for the ^{13}C(d, p) reaction [71] is, as expected, very small ($S = 0.06$). It is also not seen in the ^{13}C(n, n) data [79]. The level is strongly populated in ^{11}B(^{6}Li, ^{3}He) [55], ^{11}B(^{7}Li, α) [55], ^{12}C(α, 2p) [80, 81], and in ^{12}C(^{12}C, ^{10}C) [78], ^{12}C(t, p) [82–84] and ^{12}C(^{10}B, ^{8}B) [76] reactions. Its configuration $(d_{5/2})^2$ coupled to the ^{12}C core is discussed in refs. [54,62,82,83]. In the measurement of the ^{9}Be(^{6}Li, p) reaction [56], the $2J_f + 1$ rule was not met, as it was for most of the other states. The state may thus have also a strong-clustering component.

11.66, 4⁻ and 11.73 MeV, (4⁺), weak
Two states are listed in the compilations, they are well seen but not separated in 2n-transfer. They are well separated in our ^{9}Be(^{7}Li, d) reaction. The 4^- configuration is well established for one of the states (11.7 ± 0.1 MeV); in the tables this is the 11.666 MeV state. In the ^{13}C(p, π^-) reaction there is a sequence of states $(2^-, 3^-, 4^-, 5^-)$, which are due to core excitations of protons. The other state, at higher excitation energy of 11.730 MeV is considered to be a 4^+ state with a possible $p_{1/2} \otimes f_{7/2}$ (or $d_{5/2} \otimes d_{3/2}$) configuration.

12.58 MeV, (3⁻), weak
This state may appear as a shoulder on the stronger 12.96 MeV peak in the 2n spectrum. In the higher-resolution spectra it appears as a broad state, rather weakly populated in the triton transfers on ^{11}B, but very strong in the ^{5}He transfer on ^{9}Be. In the work of Mordechai *et al.* in the (t, p) reaction [83], this appears as a typical case with angular distributions characteristic of two-step (via 2^+) processes, and thus the DWBA calculations do not give correct spin assignments. These facts suggest that this state is a cluster state, with prolate (and not oblate!) deformation.

12.86 MeV and 12.96 MeV, (3⁻), medium
A peak corresponding to these states is well observed in 2n-transfer reactions, although not as strong as the neighboring states. In the spectrum for the ^{5}He transfer (fig. 9) and in the triton transfer (fig. 8) there are two peaks separated by 100 keV, 12.863 MeV, and 12.963 MeV, equally strongly populated. Their narrow width suggests that they are core-excited states; with the ^{12}C(2^+) state we can form a 3^- one, like in the case of the 9.80 MeV state. One of the states (or both) are populated in inelastic α-scattering. In the 2p pick-up a structure appears at 12.7 MeV incorporating possibly 3 states. The structures of these states are not clear (see also sect. 5.3).

14.0 MeV, (3⁺), weak
This state appears as a weak peak in 2n-transfer reactions, and it is covered partially by contaminants in the ^{9}Be(^{7}Li, d) reaction and observed as a rather broad peak in triton transfer reactions. The energy position fits well for the predicted $(p_{1/2}f_{7/2})_{4^+}$ but also for the $(d_{3/2}d_{5/2})_{3^+}$ configurations. However, the observation of a peak at this energy in the 2p pick-up suggests that there is also a state with core excitation. It is well separated and relatively strong in the (^{14}N, ^{12}N) reactions, suggesting unnatural parity, with a $p_{3/2}$ proton excitation. Broad structures are seen at this excitation energy in the ^{13}C(p, π) reaction [17,18] and in the triton transfer reactions [55,54].

14.67 and 14.87 MeV, (6⁺, 5⁻), very strong
These states form a strong peak in 2n-transfer reactions. The region contains at least two states as can be seen in the better-resolution spectra of the ^{9}Be(^{7}Li, d) reaction, (where the contaminant line also appears), and the states are well separated in the ^{11}B(^{6}Li, t) and the ^{11}B(^{4}He, p) reactions. The 14.87 MeV state is observed in the (p, π) reaction [17,18] and is there uniquely assigned as a 5^- state. The state is the analog of a 5^- state in ^{14}N, it can clearly be described as a core excitation and is considered to have a configuration ^{12}C(2^+) $\otimes$ $(p_{1/2} \otimes d_{5/2})_{3^-}$ with the core in

the 2^+ state (also with proton excitations). In addition, we expect mixing with the $(d_{5/2} \otimes f_{7/2})$ configuration as a neutron excitation. The latter explains the strong population in the 2n-transfer.

The 14.67 MeV state is not well separated, but only weakly populated in 2n-transfer; it is well observed in the reactions on ^{11}B as well as in the reaction on ^{9}Be as mentioned before. With its energy position compared to that observed in 2p-stripping (fig. 6 at 14.1 MeV in ^{14}O), it was proposed to be the analog state with the assignment as the $(d_{5/2}d_{3/2})_{4^+}$ configuration. We can state that it is not the $(d_{5/2}d_{3/2})_{4^+}$ state, which should be well populated in 2n-stripping, but must be a state with core excitation, a cluster state. In the triton transfer spectra, it is well separated and not strongly populated; there this state is marked as the 6^+ member of the prolate band. From the present discussion we conclude that the assignment in ref. [48] must be questioned; the strongly populated state observed there is most likely the 5^- state as an analog of the 14.87 MeV state in ^{14}C.

15.75 MeV, (2^+), weak
This state is barely seen in most reactions, however, it seems to be populated in the 2p pick-up reaction; there a strong broad structure in the range 15.2–15.9 MeV is observed. It is observed in the inelastic (π, π) reactions [85, 86]; at 15.6 MeV a wide relatively strong peak is seen in the ^{14}C(π^+, π^+) reaction [86], suggesting proton core excitation. This is a candidate for the 2^+ state obtained in the recent calculations for Gamov-Teller transitions, it is the second $2^+(p_{3/2})^{-2}$ configuration appearing at higher energy [52].

16.43 MeV, (6^+), weak
This state appears as a weak shoulder in 2n-transfer reactions, (it is separated in the (^{14}N, ^{12}N) reaction) but appears very strong in all multi-nucleon transfer reactions, also in the ^{9}Be(^{7}Li, d) reaction. It is one of the strongest states in the two reactions involving triton transfer in particular in the ^{11}B(^{6}Li, ^{3}He) reaction [55]. Its strong population in reactions with negative Q-value also points to a high spin, it is suggested to be the 6^+ state of the oblate band. There is no state at this energy in the 2p pick-up, a fact which strongly suggests that this is a cluster state with high spin. In a more recent study by Soić *et al.* [87] this state is very prominent among the states decaying into $\alpha + {}^{10}$Be.

16.72 MeV, (6^-), strong
This state is well populated in the 2n-transfer reaction. From the arguments given below, the original spin assignment of 1^+ has to be considered to be wrong, or there is an underlying second state. Andrews *et al.* [54] found a state with an angular distribution for the ^{11}B(α, p) reaction which is dominated by a $j = 9/2$ transfer. In the 2n-transfer reactions it appears only 1 MeV below the predicted energy for the $(d_{5/2}f_{7/2})_{6^-}$ state, this assignment is supported by the fact that it is not observed in the 2p pick-up, nor in reactions involving pions. We list it in table 4 also as a candidate for a core-excited state. In our ^{9}Be(^{7}Li, d) reaction we have a strong peak for this state at 16.715 MeV, but it is not seen (or very weak) in the triton transfer reaction ^{11}B(^{6}Li, ^{3}He) of ref. [55]. Both reactions are not expected to populate low-spin states, because of the large angular-momentum mismatch due to the very negative Q-values involved at this excitation energy. Due to its unnatural parity it cannot be (and was not) observed in the decay study into $\alpha + {}^{10}$Be of ref. [87].

17.5 MeV, weak
This state is only weakly observed in one of the 2n-transfer spectra, and in the (^{7}Li, d) reaction. There is in ref. [86] a 4^- state is assigned to a state at 17.3 $(+/-)$0.1 MeV. The latter is also seen as weak structure in the (^{7}Li, d) reaction. In fact it is not seen in the decay study in ref. [87] pointing to unnatural parity.

18.4–18.6 MeV, weak
This broad structure may involve several states, it is generally weaker than the low-lying peaks. It is well seen in 2n-transfer, and also as a group of states in the ^{9}Be(^{7}Li, d) reaction. In the former reaction it may be populated by higher-order processes. The energy would fit with the non-stretched $(d_{5/2}f_{7/2})_{5^-}$ configuration, with the spin coupling to a lower spin. The population of the states (one narrow, one broad) in the (p, π^-) reactions [17,18] and in the (π, π) reactions [85,86], indicates core excitation of protons. Their systematics would suggest that the narrow state within this group is potentially a 6^- state. A broad state at 18.5 MeV is also observed in a recent study by Soić *et al.* [87], where a decay into $\alpha + {}^{10}$Be(2^+) as well as into ^{10}Be(2^+) is observed.

19.8 MeV, (2^+), weak
This state again has a comparably narrow width for its high excitation energy, it is well seen, but weakly populated. It is not populated in 2p pick-up, and it fits in energy with the predicted $(d_{3/2})^2$ configuration. A weak peak is also seen in the ^{9}Be(^{7}Li, d) reaction, the low cross-section can be explained with its low spin.

21.4 MeV, (4^-–7^-)
This state (or group of states) is very conspicuous in our 2n spectra, and has also been observed in the ^{11}B(α, p) reaction [88] and as broad peak in the (p, π^-) and (π, π) reactions. This "state" may have a multiple structure, which is also not resolved in our case. The centre is unusually narrow, so we may consider that there is a state with high spin (core-excited state), and a wider structure of more simple structure like $(f_{7/2})^2$. The core excitations may be with configurations as $(d_{3/2}, f_{7/2})_{5^-}$ plus the core in a state of 2^+. If we take the pure two-neutron configuration the lower spin of the structure $(d_{5/2}f_{7/2})_{4^-}$ would also explain an additional state with a larger width at this energy. The latter would be supported by the fact that it is observed as a broad structure in ^{14}C(π^+, π^+), where the last strong narrow peak indicated as 4^- is at 17.4 MeV [86]. We also see

the population of this structure as a broad state in the ^{9}Be(^{7}Li, d) reaction and in the decay study of ref. [87] from the ^{7}Li(^{9}Be, ^{14}C $\rightarrow$ ^{10}Be + α) reaction. In the latter it is only well seen in the decay to $\alpha + {}^{10}\mathrm{Be}(2^+)$, but the ground-state decay cannot be excluded.

23.5 MeV
This structure is well seen in one of our 2n spectra, and it is also observed as a narrow peak in the ^{11}B(α, p) reaction (at an energy of 23.29 MeV) [88], there they indicate that the highest possible spin can be obtained by a mixed proton-neutron configuration like $(p_{3/2})^{-1}(\pi d_{5/2}\nu d_{5/2})_{8^-}$ so we can consider it to be a core-excited state.

We conclude that the high-lying states (above 18 MeV excitation) observed in the 2n-transfer are consistently observed also in the (^{7}Li, d) reaction and partially in the (α, p) reactions. Some of the states are further seen in the recent study of states in ^{14}C, observed through their ^{10}Be + α decay [87]; in this work, however, their widths cannot be deduced because of an overall energy resolution of $\approx$ 0.5 MeV. Actually, the states at 21.4 and 23.29 MeV are very narrow in the (α, p) reaction at $E_{\mathrm{lab}}(\alpha) = 48$ MeV [88].

4.2.2 Proton excitations from p-shell

In addition to the states with neutron single-particle structure listed above, there are low-lying states which correspond clearly to *proton excitations*. The $^{12}\mathrm{C}^*_{2^+}$ state is a proton or neutron excitation from the $p_{3/2}$- to the $p_{1/2}$-shell. Similarly the $^{12}\mathrm{C}^*_{3^-}$ state can be considered as a proton excitation from the $p_{3/2}$- to the $d_{5/2}$-shell. The states in ^{14}C based on the proton excitations of the core are very weak in neutron transfer reactions (there they would be populated by a two-step process), but strongly populated in one-proton pick-up reactions, like in the ^{15}N(d, ^{3}He) [72] and in our two-proton pick-up (fig. 6) and in the ^{16}O(^{6}Li, ^{8}B) [89] reactions. Below we discuss only some of these states individually, and on the left side of fig. 10 the remaining states are shown. Their properties are discussed with the 2n-transfer and the (^{7}Li, d) reaction.

7.012 MeV, 2$^+$
This is the strongest peak in the ^{15}N(d, ^{3}He) [72] ($C^2S = 1.13$) and ^{16}O(^{6}Li, ^{8}B) [89] reactions. It is also very strong in the ^{14}C(p, p$'$) [73] and ^{14}C(^{3}He, ^{3}He$'$) [74] inelastic scattering. It is not observed in the ^{13}C(d, p) [71] reaction, but it is rather strong in the ^{14}N(d, ^{2}He) reaction [90]. As the ground state, it also has a non-negligible amount of $(sd)^2$ strength responsible for its population in the ^{12}C(t, p) reaction [82–84]. The ^{5}He transfer reaction shows a strong population (see fig. 9 and table 3), implying that these states with proton excitation have a strong-clustering component.

11.306 MeV, 1$^+$
From the ^{13}C(n, n) data [79,91], it is suggested that this state has positive parity with probably $J^\pi = 1^+$. It is not observed in the ^{12}C(t, p) reaction [82–84]. Kaschl *et al.* observed in the ^{15}N(d, ^{3}He) proton pick-up reaction a strong 1^+ state at 11.29 MeV with a width of 150 keV [72]. Most of the strength of the $M1$ transition from the ^{14}C(e, e$'$) study was concentrated in this state [92]. Thus, the assignment with 1^+ appears very likely. The spin 1^+ thus can only be obtained by mixed proton-neutron excitation. Again this state is strongly excited (considering its low spin) in the ^{5}He transfer reaction, according to fig. 9 and table 3.

11.66 MeV, 4$^-$
Studies of (π^+, π^+) as well as (π^-, π^-) inelastic scattering [85,86] have shown that they populate states with proton excitations (2^+ or 4^-). The (π^-, π^-) reaction has a particular selectivity to 4^- states. The 11.66 MeV state is well observed in the (π^-, π^-), as well as in the ^{13}C(p, π^+)^{14}C [17,18] reaction. In the latter a multiplet is observed which could be assigned to the 3^- (9.80 MeV), 4^- (11.7 MeV) and 5^- (14.87 MeV) states, which are all formed via the $^{12}\mathrm{C}(\pi; 2^+) \otimes (\nu p_{1/2} d_{5/2})_{3^-}$ configuration.

17.3 MeV, 4$^-$
The 4^- state at 17.28 MeV is described as a proton excitation from the $p_{3/2}$- to the $d_{5/2}$-shell [54], therefore it cannot be seen in our 2p pick-up (or it can be only weakly populated through the *sd*-shell admixtures in the ^{16}O ground state), and also not in the 2n-stripping reaction.

4.2.3 Summary of the results on the reaction data

We can summarise with some general statements the different selectivity in the population of states. Many states are seen in the 2n-transfer on ^{12}C, because the reaction can strongly populate *oblate* states, due to their parentage to the ^{12}C core. The strongly populated oblate states have been listed in table 1, together with the predictions for the stretched configurations using eq. (2). Weaker populations occur for higher orbits like $d_{3/2}$, and $f_{7/2}$, as well as for two-step processes via core excitations. Some of the states with core excitations are expected also to be seen with the 2p pick-up from ^{16}O; these are again expected to be mostly oblate states, but no population of the mentioned higher orbits ($d_{3/2}, f_{7/2}$) is possible in this reaction.

The high-lying states with core excitations and neutrons in the *d*- and *f*-shells are expected to belong to the *prolate* bands and to be mixed with cluster states. This will be discussed further below.

The states in ^{14}C can be ordered into a sequence of increasing complexity (and rising excitation energy). The low-lying states with positive parity are based on the $^{12}\mathrm{C}_{0^+}$ and the $^{12}\mathrm{C}^*_{2^+}$ core and the neutrons can occupy three different shells ($p_{1/2}, s_{1/2}, d_{5/2}$), these configurations will mix to form for example three 0^+ states (at 0.0, 6.589 and 9.746 MeV), with rather different intrinsic

shapes. The lowest shell model states have overlap with oblate cluster states, which are expected to form rotational bands. The configurations for the lowest negative-parity states will be (1p-1h), namely one $p_{1/2}$ neutron promoted to the (sd)-shell. Creating a proton (π) or neutron (ν) hole in the $p_{3/2}$-shell will also give rise to negative-parity states, $(p_{3/2})^{-1}(sd)^1$, but at higher excitation energy. These states can be identified as states built on the $^{13}\mathrm{C}(3/2^-)$ state, see fig. 10, or on the $^{12}\mathrm{C}^*_{2^+}$ state. Such configurations will have (multi-particle–multi-hole) structure like $(p_{3/2})^{-1}(p_{1/2})^{-1} \otimes (sd)^2$ for positive parity for either proton or neutron configurations. With the proton excitation we can than have again three states with spin 2^+, based on different mixing of $(p_{1/2})^2$, $(s_{1/2})^2$, $(d_{5/2})^2$ configurations, as for the case of the 0^+ states.

In our attempt to obtain a complete spectroscopy we may assume that only very few states of single-particle character are missing. In fig. 10 we have summarised the present findings. We follow the guideline that the "remaining" states are related to multi-particle excitations and to clustering and larger deformations. Such states should fall into classes of oblate or prolate rotational bands, their band heads being close to the different cluster decay thresholds as discussed in the introduction.

However, for the complete spectroscopy of ^{14}C, we face the problem that there will be mixing of the cluster states with more complicated shell model configurations. There are also many levels with uncertain structure or spin assignments, which have not been placed into rotational bands.

In the excitation region above 12 MeV we observe peaks in several spectra (of the reactions 2n-stripping and $(^7\mathrm{Li}, \mathrm{d})$) which correspond to new unassigned states which we do not classify. The positions of some of these states from the $(^7\mathrm{Li}, \mathrm{d})$ reaction agree very well with those observed with the (α, p) reaction [54]. These states give room for further studies, for states obtained through coupling of the α-particle with the first 2^+ state in ^{10}Be, or more generally for states with rotational and vibrational couplings which will give rise to side bands as suggested in ref. [93].

4.3 Discussion of the states with oblate deformation

After having discussed the states populated in different reactions we want to localise states with oblate shapes and cluster character.

The cluster states in ^{14}C are related to multi-particle–multi-hole excitations, like the 4p-2h structures for the 0^+_2 (see also ref. [57]). The excitation of protons naturally produces a α-^{10}Be configuration, which can give rise to oblate ("pancakes") or prolate shapes (chain configurations). We expect in the lowest-energy range mainly the oblate shapes. We are particularly interested in the interpretation of the states around ≈ 10 MeV excitation energy and higher. Our compilation (tables 1, 2 and 3 and fig. 10) helps us to identify excited states with cluster structure. Some of these states are similar to the "normal oblate states" in ^{12}C, like the 0^+_1 and 2^+_1. More interesting states of ^{12}C are the 0^+_2 state at 7.65 MeV and the 3^-_1 state at 9.64 MeV; these show clear cluster nature and are not reproduced by the largest shell model calculations [94]. Corresponding levels in ^{13}C are discussed in the literature to be predominantly $p^7(sd)^2$ in character and possibly arising from the coupling of two nucleons in the lowest sd-shell Nilsson orbit to the ground state $(K = 3/2)$ and the first-excited state $(K = 1/2)$ bands of an $A = 11$ core [95]. A strong population of the oblate states in ^{14}C with $p^7(sd)^3$ configurations in three-nucleon transfer reactions on ^{11}B must thus be expected.

Table 5. Proposed *oblate* or "triangular" bands in ^{14}C. The indices indicate the population in certain reactions, "a", $(^7\mathrm{Li}, \mathrm{d})$, and "b", inelastic scattering, "c", 2p pick-up, "d", in (α, p), in the (p, π) and in "2n" reactions.

J^π Proposed	E_x (MeV)	J^π Ref. [51]	Population	Γ or τ (keV)
$K = 3^-$				
3^-	9.801	3^-	a, b, c, d, 2n	45
4^-	11.67	4^-	a, d	20
5^-	14.87	$(6^+, 5^-)$	a, b, d, 2n	35
$K = 0^+$				
0^+	6.589	0^+	a, b	3 ps
2^+	8.318	2^+	a, b, c, 2n	3.4
4^+	10.74	4^+	a, 2n	20
6^+	16.43	–	a, 2n	35

The 0^+_2 state at 6.59 MeV of ^{14}C is often described [68] by an orthogonalization to the ground state 0^+_1, the two states are mixed due to a pairing interaction in their 2n-configurations in the p-, and sd-shells, $^{12}\mathrm{C}(0^+_1) \otimes [a(p_{1/2})^2 + b(s_{1/2})^2 + c(d_{5/2})^2]$. This situation will give three new states. The amplitudes a, b, c have been discussed in the literature, and have been recently used in 2n-transfer calculations with very good results [70]. These configurations can be compared to the $^{12}\mathrm{C}(0^+_2)$ state, which has no definite shape, but is expected to be oblate. Actually Itagaki *et al.* [4] predict the "triangular" state in ^{14}C with spin/parity 0^+ at 7.85 MeV of excitation energy, very close to the observed energy of the 0^+_2 state at 6.589 MeV. This indicates that this state is strongly related to the 0^+_2 in ^{12}C and to the special states with spin/parity of $1/2^-$ and $1/2^+$ at 8–10 MeV of excitation in ^{13}C, discussed in refs. [8–10]. For the "triangular" 0^+ states no particular orientation can be defined for the third α-particle. Due to the spin zero their intrinsic density is not "triangular", but is described by any relative orientation of the three α-particles. For a state with a fixed "triangular" geometry, excited states in ^{12}C and ^{14}C with a spin of 3^- are expected [96,93]. For ^{14}C it is most likely the 3^-_2 state at 9.801 MeV predicted also by Itagaki *et al.* at 9.45 MeV [4]. In the spectrum of the ^{5}He transfer this 3^-_2 state is separated and well populated, as well as the 8.32 MeV (2^+_2) state, and the other members of the $K = 0^+$ and $K = 3^-$ bands. The two latter are only weakly seen in the 2n-transfer spectrum.

We are thus able to propose the two oblate rotational bands in ^{14}C, as summarised in table 5 and figs. 11 and 12.

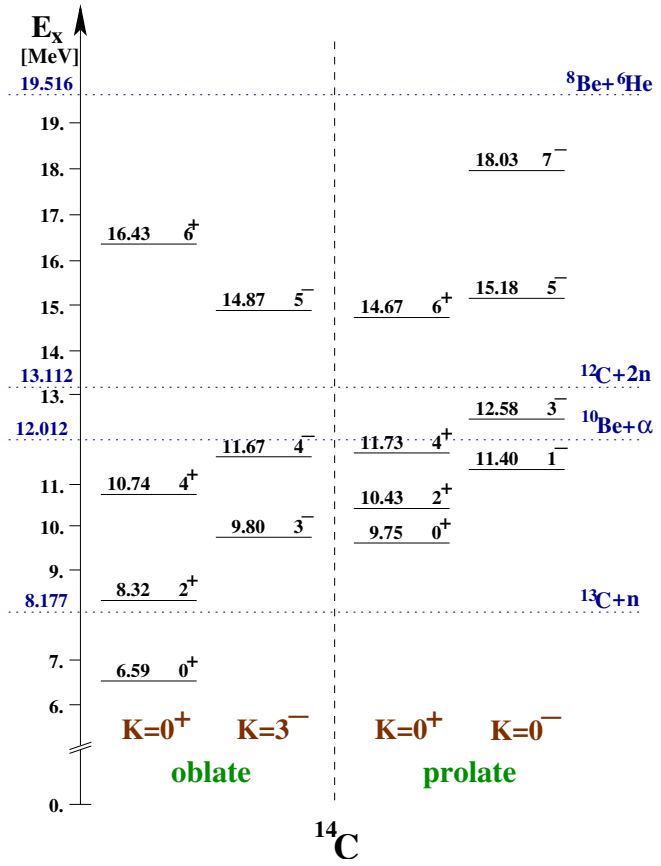

Fig. 11. Energy levels with their proposed spins selected from the population characteristics to form rotational bands. The states are used to build bands with K-quantum numbers as indicated. The spin assignments are discussed in the text. Thresholds for various structure components of states in ^{13}C and ^{14}C, related to the asymptotic basis of states like $(\alpha + \mathrm{Be})$ are shown.

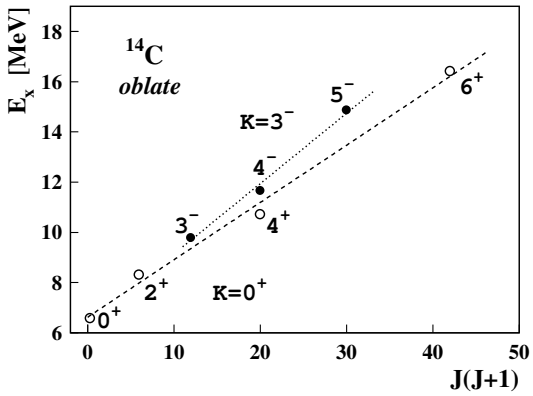

Fig. 12. Proposed oblate α-cluster bands in ^{14}C. These are states, which cannot be attributed to single-particle states based on low-lying states of ^{12}C (g.s., 2_1^+ and 1_1^+). Their energies are plotted as a function of their assumed spins, $J(J+1)$, forming rotational bands with K-quantum numbers as indicated.

The moments of inertia are obtained from the fits to the excitation energies for these bands, the parameters are $(\hbar/2\theta) = 250\,\mathrm{keV}$ and $290\,\mathrm{keV}$ for the $K = 0^+$ and $K = 3^-$ bands, respectively. The low-lying states of these bands are well populated in inelastic scattering, in the triton transfer as well as in our $(^7\mathrm{Li}, \mathrm{d})$ reaction.

We proceed to discuss the properties of the individual states proposed for these two bands.

4.4 The oblate K = 0$^+$ and 3$^-$ bands

4.4.1 The oblate $K = 0^+$ band

6.589 MeV state, 0_2^+

This 0_2^+ state is strongly populated in the $^9\mathrm{Be}(^7\mathrm{Li}, \mathrm{d})$ reaction (fig. 9), in particular considering its low spin. It is not seen either in one-nucleon transfer reactions $^{13}\mathrm{C}(\mathrm{d}, \mathrm{p})$ [71] ($S < 0.18$) nor in $^{15}\mathrm{N}(\mathrm{d}, ^3\mathrm{He})$ [72]. It is also not seen in proton [73] and deuteron inelastic scattering. It was seen in an early $^9\mathrm{Be}(^7\mathrm{Li}, \mathrm{d})$ measurement [97], and is proposed to have $(sd)^2$ configurations for the two neutrons as already noted by Fortune [62].

8.32 MeV state, 2_2^+

This 2_2^+ state is strongly populated in the $^9\mathrm{Be}(^7\mathrm{Li}, \mathrm{d})$ reaction (fig. 9), but comparably (in comparison with the 4^+ state) weakly populated in the 2n-transfer reactions (see fig. 4). We have already mentioned that it has a strong proton component, because it is seen in the 2p pick-up, with proton excitations from the $p_{3/2}$-shell. It is rather strong in many reactions, like $^{14}\mathrm{N}(\mathrm{d}, ^2\mathrm{He})$ [90], $^{12}\mathrm{C}(\alpha, ^2\mathrm{He})$ [80,81], $^{13}\mathrm{C}(\mathrm{d}, \mathrm{p})$ [71], $^{15}\mathrm{N}(\mathrm{d}, ^3\mathrm{He})$ [72], as well as in inelastic scattering $^{14}\mathrm{C}(\mathrm{p}, \mathrm{p}')$ [73], $^{14}\mathrm{C}(\mathrm{d}, \mathrm{d}')$ [77], $^{14}\mathrm{C}(^3\mathrm{He}, ^3\mathrm{He}')$ [74], $^{14}\mathrm{C}(\alpha, \alpha')$ [71] and $^{16}\mathrm{O}(^6\mathrm{Li}, ^8\mathrm{B})$ [89] reactions. It is also populated in the $^{14}\mathrm{C}(\pi^+, \pi^{+\prime})$, but not (!) in the $^{14}\mathrm{C}(\pi^-, \pi^{-\prime})$ reaction [85,86]; the latter reaction emphasizes stretched configurations with unnatural parity. This fact must be interpreted that it is a proton excitation, which can imply in our picture a (6p-4h) configuration. Its more complicated structure is confirmed by the fact, that in calculations with a shell model basis space restricted to the p-shell [58], just one low-lying 2^+ state at 7.13 MeV is predicted, with the second 2^+ state much higher at 15.19 MeV. So, the structure of the lower-lying state at 7.012 MeV corresponds to excitations within the p-shell, whereas the 8.317 MeV state is expected to involve components with higher shells. The 8.317 MeV state is proposed to have a $(sd)^2$ character also in ref. [62]. Those two states show markedly different population in some reactions. For example, pion scattering data [85,86] show almost equal $(\pi^+, \pi^{+\prime})$ and (π^-, π^-) cross-sections for the 7.012 MeV state, while $(\pi^+, \pi^{+\prime})/(\pi^-, \pi^-)$ cross-section ratio is huge (> 26) for the 8.317 MeV state. Angular distributions for these two states are also often very different (*e.g.* [71,85,86]).

10.74 MeV state, 4^+
This state is well separated and strongly populated in the ^{9}Be(^{7}Li, d) reaction. From the spectra in fig. 4 we conclude, that it is also strongly populated in the 2n-transfer reaction, (but not separated from states at 10.43 and 10.49 MeV). It is populated again in (π^+, π^+), but not in (π^-, π^-) [85,86]. It is also populated and well separated in ^{11}B(^{6}Li, ^{3}He) and ^{11}B(^{7}Li, α) reactions [55].

16.43 MeV state, (6^+)
This state is a good candidate for the highest spin, with a narrow width, well separated and strongly populated in the ^{9}Be(^{7}Li, d) reaction. In the 2n-transfer reaction the configuration for 6^+ is difficult to populate as it needs an excitation of the ^{12}C core, it is weakly populated in one of the 2n-transfer reactions. Consistent with this interpretation the level is very strongly populated in the triton transfer reactions like ^{11}B(^{6}Li, ^{3}He) and ^{11}B(^{7}Li, α) [55]. These observations suggest high spin and an oblate shape (and core excitation).

This cluster band could have higher-spin members; however, considering weak coupling of two neutrons to an excited ^{12}C*, a maximum spin is obtained with the $2^+ \otimes (d_{5/2})^2$ configuration. The irregularities in the energy sequence observed for these bands as well as the following bands may point to the suggested configuration mixings, which can shift the energies of individual states.

4.4.2 The triangular $K = 3^-$ band

9.801 MeV state, 3_2^-
The 3^- assignment is based on the ^{14}C(p, p′) measurements [51]. This second 3_2^- state is strongly populated in the ^{9}Be(^{7}Li, d) reaction, as shown in fig. 9. Andrews *et al.* [54] suggest a $\nu d_{5/2} \otimes {}^{13}\mathrm{C}_{3/2^-}$ configuration for this state. The (n, n) reaction analyzed by Lane *et al.* [79, 91] suggests (from the R-matrix analysis of the ^{12}C(n, n) reaction) that there are actually two states near this excitation energy. In the work of Wendler *et al.* [98] a 1^- state at 9.789 MeV and a 3^- state at 9.806 MeV are given. The latter is also the candidate for the 3_2^- state in the (t, p) reaction of ref. [56]. This state (or the two states?) is the strongest one in (α, α') scattering [71]. On the other hand, it is barely visible in the ^{13}C(d, p) reaction [71], these results are in favor of a collective state with strong clustering.

11.67 MeV state, 4^-
A state at 11.67 MeV was first reported by McGrath [99] using the ^{11}B(^{7}Li, α) reaction. This state with unnatural parity is very strong in inelastic π^--pion scattering and is unambiguously assigned as 4^- [51]. It is strongly populated in the ^{9}Be(^{7}Li, d) reaction (fig. 9). It is only weakly excited in the 2n-transfer reactions shown in figs. 4, (as well as in ref. [51]), where it is unresolved from another weakly populated high-spin state. A 4^- assignment was based on the excitation functions and differential cross-sections of the ^{14}C($\pi^\pm, \pi^\pm$) reactions [85,86] (Clark and Kemper [55] suggest that this state is populated in the pion scattering and labeled as the 11.73 MeV state). It is very strong in the ^{13}C(p, π^+) reaction [17,18]. The configuration suggested there is $^{12}\mathrm{C} \otimes (\nu p_{1/2})^2$, $(\nu p_{3/2})^{-1}$, $(\nu d_{5/2})$, where the $(\nu p_{3/2})^{-1}$-hole could also be a proton hole $(\pi p_{3/2})^{-1}$. Also, the electron scattering data [100, 101] suggest a 4^- state at 11.72 MeV. So it is not clear if another state is to be found in the vicinity. This state is not observed in the ^{13}C(n, n) reaction [79,91]. All results are in favor for a cluster state.

14.87 MeV, (5^-)
There is a proposed 6^+ state at 14.67 MeV close by, whose characteristics are discussed later with the prolate bands (see the next section), which is not populated in 2n-transfer reactions, there it is usually not well resolved from the state at 14.87 MeV. Both states are strongly populated and well separated in the ^{9}Be(^{7}Li, d) reaction. These states are very strong (and resolved) in the ^{11}B(^{6}Li, ^{3}He) reaction, while the second is much stronger in the ^{11}B(^{7}Li, α) reaction [55], indicating a lower spin (because of the much more positive Q-value compared to the (^{6}Li, ^{3}He) reaction). In refs. [76,81] it is suggested to have $(d_{5/2}d_{3/2})_{4^+}$ character. The latter is very strongly populated in our 2n-transfer reactions. The 14.87 MeV state is probably the state seen in the ^{12}C(^{10}B, ^{8}B) reaction at 15.0 MeV [76] and it is rather strong in the ^{12}C(α, ^{2}He) reaction [80,81], so this state appears in table 4 with the 2n-configurations. The negative-parity state is very strong in the ^{14}C(p, π^+) as well as in the ^{14}C(p, π^-) reaction [17,18]. There a $J^\pi = 5^-$ spin value is assigned to this state on the basis of its strong excitation also from comparing it to the ^{14}O (14.15 MeV) and ^{14}N (16.91 MeV) analog states. The configuration is therefore suggested to involve a proton excitation $^{12}\mathrm{C} \otimes (\pi p_{3/2})^{-1}$, $(\pi p_{1/2})^1$, $(\nu p_{1/2})$, $(\nu d_{5/2})$, but also the equivalent neutron excitation can be possible to form 5^-. We can form this state with a 1p-1h excitation using the 2^+ state in ^{12}C (this state coupled with a 3^- configuration). The 5^- state is proposed to belong to the present band.

The $K = 3^-$ band may terminate with $J^\pi = 5^-$ as suggested by the shell model picture (see also Itagaki *et al.* [4,5]); however, in the cluster model the band would continue, a candidate for the (6^-) state can be found at 18.4 MeV well populated in 2n-transfer and in other reactions.

4.5 Prolate deformed bands or chain states of ^{14}C

After the preceding compilation, there are many more states at the higher excitation energy in ^{14}C, which we expect to be connected to cluster states with prolate deformations. Inspecting these remaining states in the vicinity of the α-^{10}Be threshold, we expect the states to form rotational bands as inversion parity doublets, like in ^{13}C (see ref. [8]). As already suggested the structure will be strongly influenced by the pairing interaction and the neutrons remain concentrated with two of the centres. Thus, the linear structure must be connected to the intrinsic

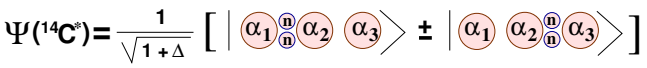

Fig. 13. Schematic illustration of linear chain configurations in ^{14}C forming a parity inversion doublet with $K = 0^{\pm}$; bands are starting close to the α-^{10}Be threshold.

Table 6. Proposed *prolate* parity split bands (chain states) in ^{14}C. The label "a" indicates very strong, "x" stands for normal, population in the ^{9}Be(^{7}Li, d)^{14}C reaction.

J^π proposed	E_x (MeV)	J^π ref. [51]	Population	Γ or τ (keV)
$K = 0^-$				
1^-	11.395	1^-	x	22
3^-	12.58	$(2^-, 3^-)$	a	95
5^-	15.18	(4^+)	x	50
(7^-)	18.04	–	x	70
$K = 0^+$				
0^+	9.75	0^+	x	≤ 4
2^+	10.43	2^+	x	≤ 35
4^+	11.73	(5^-)	x	≤ 35
6^+	14.67	$(5^-, 6^+)$	x	40

reflection-asymmetric ^{10}Be + α configuration. The parity projection is illustrated in fig. 13. We can propose the existence of two parity split rotational bands with $K = 0$ (as given in table 6 and illustrated in fig. 14).

The energy splitting between the positive- and the negative-parity bands must be expected to be similar to that of the $K = 3/2$ parity spin doublet band in ^{13}C. Figure 14 shows the plot of excitation energies of the states from fig. 11 as a function of $J(J + 1)$.

All states of the chain configuration are not so strong in the triton transfer reactions, but all are well observed in the ^{9}Be(^{7}Li, d) reaction (fig. 9). In the remaining part of this section we will give arguments for putting each of the states into the proposed bands.

4.5.1 The prolate $K = 0^+$ band

9.746 MeV, 0_3^+
This is the third state with $J = 0$, it was first observed as a very weak peak by Mordechai *et al.* [82] in the ^{12}C(t, p) reaction. It was also seen in the ^{11}B(^{6}Li, ^{3}He) reaction [55]. There is no indication of any neutron resonance near this excitation energy [79]. Also, it is not seen in single-nucleon transfer reactions. This is not surprising since this state is expected to be predominantly described in terms of two neutrons in the *sd*-shell coupled to the ^{12}C core according to refs. [60,62]. It is probably populated in the ^{9}Be(^{7}Li, d) reaction, but not well separated from the strong 3_2^- state at 9.80 MeV; there is a distinct shoulder on the right side, implying a larger error in the relative-strength values in table 3. The relative weight of the 3_2^- state given in table 3 is to large also judging the other values. Their relative weights should be 80 for the (0^+) and 120 for the 3_2^-, in table 3.

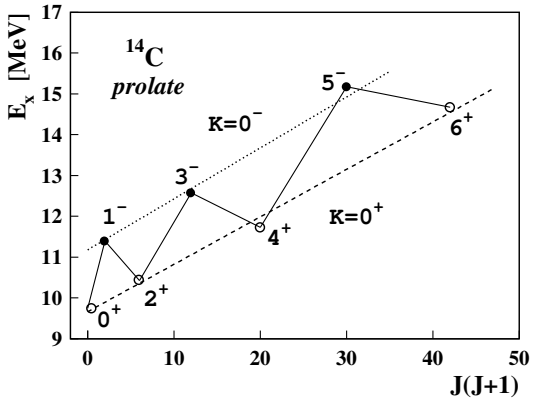

Fig. 14. Proposed prolate α-cluster bands in ^{14}C. These are states which cannot be attributed to single-particle states based on low-lying states of ^{12}C (g.s., 2_1^+ and 1_1^+), their energies are plotted as a function of their assumed spins, $J(J+1)$, forming rotational bands with K-quantum numbers as indicated.

10.43 MeV, 2^+
A strong state has been observed in the (t, p) reaction at this energy, for which an assignment of $J^\pi = 2^+$ was given. There are two states observed in this energy region, whose energies are quoted slightly differently in two subsequent works [56,84]. In our analysis we have initially used three states. We give in table 3 two states at 10.42 and 10.49 MeV. For the first state, the assignment of $J^\pi = 1^+$ gave the best fit to the resonance in the ^{13}C(n, n) data, although $J^\pi = 2^\pm$ could not be excluded [79]. It is very strong in the ^{15}N(d, ^{3}He) reaction. It is also strong in the ^{16}O(^{6}Li, ^{8}B) reaction [89], as well as in our ^{16}O(^{15}N, ^{17}F) reaction, where mainly 2^+ states are strong. It is well populated in the ^{9}Be(^{7}Li, d), this suggests that this is a cluster state with a 2^+ spin value.

11.73 MeV, (4^+)
This state has a spin similar to that of the level at 11.67 MeV [55], both are well separated in the ^{9}Be(^{7}Li, d) reaction, and they have been discussed with the 2n-transfer. A tentative assignment of 5^- was made by Mordechai *et al.* [82], where the $(d_{5/2}f_{7/2})_{5^-}$ character has been proposed. However, as discussed with the single-particle states, the state with this assignment is most likely to be found higher at 17.7 MeV (6^-), and the corresponding (5^-) at even higher energy. It is also populated in the ^{11}B(^{6}Li, ^{3}He) reaction, but it is not seen in the ^{13}C(n, n) reaction [79,91]. The strong peak at this energy in the 2n spectrum may be rather due to the (4^-) state, already attributed to the oblate band. We suggest it to have (4^+) in view of systematics and the results already quoted before and in table 3.

14.67 MeV, (6^+)
This state could be populated in 2n-transfer reactions (via a two-step mechanism); there it is usually not resolved from the state at 14.87 MeV (which is considered to be (5^-)). Both states are strongly populated and well separated in the ^{9}Be(^{7}Li, d) reaction. These states

are very strong (and resolved) in the ^{11}B(^{6}Li, ^{3}He) reaction, while they appear weaker in the ^{11}B(^{7}Li, α) reaction [55]. The state at 14.87 MeV is probably the one seen in the ^{12}C(^{10}B, ^{8}B) reaction at 15.0 MeV [76] and it is rather strong in the ^{12}C(α, ^{2}He) reaction [80,81], which suggests that the latter is the already mentioned state with oblate shape with (5^-). The strong cross-section for the 14.67 MeV state in the ^{9}Be(^{7}Li, d) reaction suggests a higher spin, with (6^+) it would fit into the band structure and the systematics of intensities in table 3.

Again we may consider that this band does not terminate at the spin value of 6^+. A conspicuous state at 19.73 MeV or 19.8 MeV is well populated in the ^{9}Be(^{7}Li, d) and in the 2n-transfer reactions at an excitation energy fitting the $J(J+1)$ systematics.

4.5.2 The prolate $K = 0^-$ band

11.395 MeV, 1^-
In the ^{13}C(n, n) data [79], there is a very narrow resonance ($\Gamma < 7$ keV) at $E_n = 3.466$ MeV, on top of the very broad structure in the range $E_n = 3.0$–4.5 MeV. Mordechai *et al.* [82] make a strong claim that it has $J^\pi = 1^-$, in agreement with the ^{13}C(n, n) data of ref. [91]. Ajzenberg-Selove assign [56] $J^\pi = 2^+$ or 3^+ to this state. Andrews *et al.* [54] suggest 1^- and a $\nu 2s_{1/2} \otimes {}^{13}\mathrm{C}p_{3/2^-}$ configuration. It is fairly strong in the ^{9}Be(^{7}Li, d) reaction, suggesting cluster structure.

12.583 MeV, 3^-
The ^{13}C(n, n) data [79] suggest a 2^- or 3^- assignment which is also consistent with the results of the ^{12}C(t, p) reaction in ref. [82]. The $(d_{5/2}p_{1/2})_{3^-}$ character has been proposed [82]. However, from other ^{12}C(n, n) data [91], it is claimed to have a spin $J^\pi = 2^-$. But with this assignment the $2J_f + 1$ rule was not met in the measurement of the earlier ^{9}Be(^{6}Li, p) reaction [56]. In our ^{9}Be(^{7}Li, d) reaction it is strongly populated, suggesting natural parity; a spin of 3^- is needed to explain its intensity in table 3; this spin fits well into the proposed band. It appears in the 2n-transfer reactions as a shoulder next to the strong 12.96 MeV state.

15.18 MeV, (5^-)
This state is again well separated and strongly populated in the ^{9}Be(^{7}Li, d) reaction, it has a narrow width. It is seen in (π, π) reactions, but rather suppressed, compared to the 4^- states, suggesting a natural-parity state and we have placed it in the $K = 0^-$ band, where it fits well for the 5^- state.

18.04 MeV, (7^-)
In the ^{9}Be(^{7}Li, d) reaction we have a well-populated state at this excitation energy (actually with another state just below). It is not observed in 2n-transfer nor in the ^{11}B(^{4}He, p) reaction, therefore it is placed as a candidate of the prolate band at higher spin.

4.6 Mirror states in ^{14}O

For the covalent molecular cluster states the concept of isospin, which is related to a mean-field potential where in the average *all* nucleons interact with each other, loses its validity. In the loosely bound system the Coulomb energy for valence protons may become very large and push the clusters apart. Therefore we expect the disappearance in ^{14}O of some of the mirror states with configurations of delocalised proton orbitals, but also because of the lower thresholds for particle decay. The Coulomb interaction in their covalent configurations will counteract the covalent binding effect, implying that we will lose the mirror states in ^{14}O at higher excitation energy, We could thus identify some of the cluster states by a comparison of the 2n-transfer with the 2p-transfer reactions.

In ^{14}O we can observe only a few high-lying states (fig. 6), whereas we observe in the 2n reaction the population of many more states (see fig. 4). The shell model configurations with the $f_{7/2}$-orbits certainly contribute to the cluster structures; for these we expect the proton states to be unstable, even at high spin. In fact we should have expected the population of some analogs of cluster states in the 2p-transfer via two-step processes (*e.g.*, with an inelastic excitation to the ^{12}C$^*(2^+)$ state), like in the 2n-transfer reaction, where many narrow cluster states (although weakly populated) appear above 18 MeV excitation energy.

The most prominent narrow peaks reported in ref. [48] for the ^{12}C(^{12}C, ^{10}Be) reaction are at 9.90 MeV (4^+), 14.1 MeV (4^+) and 15.7 MeV (5^-) as discussed in sect. 3. The analogs in ^{14}C are interpreted as 10.73 MeV $(d_{5/2})^2_{4^+}$, 14.87 MeV $(f_{7/2} \otimes d_{5/2})_{5^-}$ and 16.72 MeV $(d_{5/2} \otimes f_{7/2})_{6^-}$ states. This would imply a systematic shift by ≈ 1 MeV to lower excitation energy for the ^{14}O configurations.

The analog states in ^{14}C and ^{14}O have also been studied in ref. [18], while comparison of those in ^{14}C and ^{14}N has been done in ref. [55].

5 Discussion and conclusions

We have made a survey of the majority of states in ^{14}C, which are strongly populated, but with very different selectivity, in reactions involving 2-nucleon transfer and cluster transfer. Although there are still some higher-lying states, whose spin/parity assignment has to be determined, we can state, that after inspection of all states with reactions of different population characteristics we can make a separate ordering of the properties of states.

5.1 Summary of the evidence for cluster chain states in ^{14}C

As a conclusion from the new experimental data and the survey of the literature we state that we have identified those levels which can be related to deformed states with cluster structure in ^{14}C, forming bands based on a pronounced $\alpha + {}^{10}$Be structure. With this structure we can

Table 7. Moments of inertia for rotational bands in nuclei with $A \approx 10$–16.

Nucleus	Band head	$\frac{\hbar^2}{2\theta}$ (keV)	References
^{10}Be	0_2^+, 1_1^-	250	dimer [1,23]
^{11}Be	$3/2_3^-$	230	dimer [24,27]
^{12}Be	0_2^+	210	[27,29]
^{12}C	g.s.	740	[51]
^{13}C	$3/2_2^-$, $3/2_3^+$	190	chain [8]
^{14}C	0_2^+, 3_2^-	230, 280	oblate, this work
^{14}C	0_3^+, 1_2^-	120, 130	chain, this work
^{14}C	0_2^+, 3_2^-	300	oblate, pred. in [4]
^{16}C	0^+	150	chain, pred. in [3]

have a linear prolate configuration with the pairing interaction for two neutrons giving a big effect. The intrinsic reflection-asymmetric structure with the ^{10}Be ground state gives rise to inversion parity doublets. The second possible linear structure with an intrinsic symmetric configuration more related to the linear chains found in ^{13}C [8] is expected at higher excitation energy with the neutrons shared with equal amplitudes among all three centres.

The bands we have identified as linear chains come in pairs, the states are parity doublets. The structure of the intrinsic shapes has been discussed in many works as given in the introduction (sect. 1). We compare the moments of inertia of the bands in ^{14}C with the moments of inertia of other molecular bands in light nuclei in table 7. The proposed bands in ^{14}C have very large values of $\hbar^2/2\theta \approx 120$ keV, consistent with the concept of chain states. These values are actually larger then those predicted for ^{16}C, a fact which could be explained by the residual pairing interaction (so far not considered for ^{16}C), which enhances and concentrates the densities of the valence neutrons at the two ends of the chain.

5.2 The oblate states of $^{13-14}$C

A different arrangement of three α-particles will give the oblate structures, with the particular feature of a triangular band with $K = 3^-$. We also remark that the moment of inertia is larger for the prolate bands, as compared to the oblate bands. This fact intuitively is expected due to the larger geometrical extension. The case of the oblate configurations, which can be more directly related to low-lying states in ^{12}C and ^{13}C appears to be rather clear. If the two neutrons are distributed as calculated by Itagaki *et al.* in ref. [4], to form states with definite parity, we can put a node in the centre of the triangle; this configuration gives a minimum spin of 3^-. For positive parity, with a maximum of the valence particles wave function in the centre we obtain a state with 0^+. This is reminiscent of the well-known states 0_2^+ in ^{12}C at 7.65 MeV and 3^- at 9.6 MeV, which are known to have a very peculiar and dilute cluster structure. It is interesting to note that large-scale shell model calculations quoted in refs. [91,100,101] cannot reproduce any of the first states of our proposed bands ($0_2^+, 3_2^-, 0_3^+, \ldots$). We suggest accordingly that there are two bands in ^{14}C with $K^\pi = 0^+$ and $K^\pi = 3^-$ with oblate configurations. These could also be based on the ^{10}Be$(0^+) + \alpha$ structure, or even more appropriate, because of considerations with the Pauli principle; they could be based with a combination of the hybridized state in ^{10}Be(1^-), at 5.96 MeV. In the latter case the neutron densities are strongly distorted, according to Kanada-En'yo *et al.* [35], and can thus favorably support the triangular shape of these oblate bands.

Because these oblate states can also be related to the oblate ground state and the 2^+ state of ^{12}C, they are well populated via two-step interactions in 2n-stripping reactions, as well as in the ^{9}Be(^{7}Li, d) reaction, as discussed in sect. 3.

5.3 Unassigned high-lying states

We have not yet reached the full account of all levels needed in a complete spectroscopy. For the states of explicit cluster structure, the symmetries of the 3-body system are of importance. To illustrate the latter point, we discuss here only shortly a recent study within the algebraic cluster model by Bijker and Iachello [93]; there the symmetries of an oblate top consisting of three identical clusters are discussed. The system has a discrete symmetry expressed as D_{3h} which consists of a rotation D_3 and a parity operation P, $D_{3h} = D_3\ P$. The parity of the bands will be determined by $P = (-)^K$, the bands will have the structure, either $L = 0, 2, 4, \ldots$ for $K = 0$, or $L = K, K+1, K+2, \ldots$. Due to this symmetry no state with dipole character and no $L = 1$ transitions should occur. Most relevant in their discussion is the question of vibrational excitations, namely the states within the cluster-cluster potential, and their coupling to rotations. The algrebaic model can in particular deal with the couplings between these degrees of freedom. Additional bands with $K \neq 0$ are obtained by vibrational excitations, with values $K = 3n+1, 3n+2$ and $J = K, K+1, K+2 \ldots$, or in our specific case via the coupling with the first 2^+ state in ^{10}Be. There are actually quite a few unassigned states mostly with unassigned spin, in the intermediate excitation energy discussed here, which eventually could fit into this scheme.

In the discussion of the bands we have left out many states at the higher excitation energies (up to 21.4 MeV) for which presently no further information can be given. We leave them to future work, certainly many new measurements of spins and the decay properties are needed to establish finally the structure of the highly excited states in ^{14}C.

The states identified as cluster states in the present work may still have rather good representation using the deformed shell model configurations. Inspecting the diagram of fig. 1 we can deduce that the valence particles on top of the three α-particles in the case of the 3 : 1 deformation, will be related to $K = 1/2$ orbits of the $f_{7/2}$-shell, which has descended to the level of the $K = 3/2$ of the p-shell. Thus the $f_{7/2}$-shell may strongly contribute to the shell model description of the proposed states forming the bands with the lower energies described in this work.

Some of the extra states at excitation energies around 18.0–22.0 MeV need further studies; however, their energy positions are in a region of the 3α+2n threshold, where the intrinsic reflection-symmetric chains are expected [1,4,6].

5.4 Final remarks

We have already mentioned, that the parity splitting of the $K = 0$ bands in ^{14}C is as strong as for the $K = 3/2$ bands in ^{13}C, but not as strong as for the 4p-4h cases in ^{16}O (first-excited 0_2^+ state) and in ^{20}Ne (see, *e.g.*, [102]). This observation must be related to the probability of the neutron transfer between the two inverted configurations of ^{10}Be and ^{4}He shown in fig. 13. As in the case of ^{13}C this exhange process would manifest itself in a strong backward rise in the elastic scattering; such a study is in preparation.

We believe that the observation of the parity split bands confirms an intrinsic structure, which, due to the pairing interaction, leads to a three-centre structure, which is different from those structures where the neutrons are shared with equal amplitudes among all three centres, discussed in refs. [8,3–5].

Finally a comment on ^{16}C; there a rather interesting case may occur which will have as the lowest shape isomeric state an intrinsically symmetric configuration with positive parity and a strong lowering of the excitation energy from the threshold. The binding energy is expected also to be increased if the pairing energy is considered. For ^{16}C we consider principal structures with four neutrons in the molecular orbitals based on the Hückel method [103] as described in ref. [8]. However, the pairing interaction will give an additional effect to the total binding energy obtained by Itagaki [3]. If we use molecular orbital configurations with different symmetries filling the two gaps between the alpha-particles again intrinsically asymmetric states will appear: for example, i) $(\pi)^2 \times (\sigma)^2$ or ii) $(\sigma \times \pi)^2$. In the latter case the neutrons are in different orbitals, and interesting hybridized configurations can be expected, and the linear chain is predicted in ref. [3] to be strongly stabilized relative to the bending mode.

We can state that the study of nuclear shape isomers in the carbon isotopes is a fascinating subject, which will reveal unusual nuclear structures. The shape coexistence of normal shell model states with oblate and prolate deformed cluster states is reminiscent of the case of ^{186}Pb, where also very different shapes are observed within a narrow range of excitation energies [104]. Actually, the states proposed for the linear chain correspond to hyperdeformation, and further work is in progress to establish a complete spectroscopy for the carbon isotopes. Multi-nucleon transfer reactions will be needed to populate the cluster states. The most effective description of these structures must be found by using explicitly molecular orbital methods. Thus, the study of these extended structures will reveal nuclear-structure physics well beyond the shell model.

We have benefitted from numerous helps during the experiments; we particularly thank the staff members of the Meier-Leibniz Laboratory, Munich, for their support. We are indebted to N. Itagaki for helpful discussions. This work has been supported by the A.v. Humbodlt foundation, the DAAD and the federal ministry of research (BMBF) under contract No. 06-OB-900, and the DFG(C4-Gr894/2-3).

References

1. W. von Oertzen, Z. Physik A **357**, 355 (1997); Nuovo Cimento A **110**, 895 (1997).
2. K. Ikeda, N. Takigawa, H. Horiuchi, Prog. Theor. Phys. (Japan), Suppl. Extra Number, 464 (1968).
3. N. Itagaki, S. Okabe, K. Ikeda, I. Tanihata, Phys. Rev. C **64**, 014301 (2001).
4. N. Itagaki *et al.*, *Proceedings of Yukawa International Seminar 2002, Physics of Unstable Nuclei*, Prog. Theor. Phys. (Japan), Suppl. **146**, 207 (2002), and private communication.
5. N. Itagaki, T. Otsuka, S. Okabe, K. Ikeda, *Proceedings of the Syposium on Nuclear Clusters, Rauischholzhausen, 2002*, edited by R. Jolos, W. Scheid (EP Systema, Debrecen, Hungary, 2003) pp. 47-52.
6. W. von Oertzen, H.G. Bohlen, C. R. Phys. **4**, 465 (2003); W. von Oertzen, Prog. Theor. Physics (Japan), Suppl. **146**, 169 (2002).
7. A. Tohsaki, H. Horiuchi, P. Schuck, G. Röpke, Phys. Rev. Lett. **87**, 192501 (2001).
8. M. Milin, W. von Oertzen, Eur. Phys. J. A **14**, 295 (2002).
9. M. Milin, W. von Oertzen, *Proceedings of the Symposium on Nuclear Clusters Rauischholzhausen, 2002*, edited by R. Jolos, W. Scheid (EP Systema, Debrecen, Hungary, 2003) p. 45.
10. M. Milin, W. von Oertzen, Fizika B **12**, 61 (2003).
11. A. Bohr, B. Mottelson, *Nuclear Structure*, Vol. **II** (Benjamin Inc., Reading Mass, 1975).
12. W. von Oertzen, Eur. Phys. J. A **11**, 403 (2001).
13. Y.K. Kanada-En'yo, H. Horiuchi, Prog. Theor. Phys. (Japan), Suppl. **142**, 205 (2001).
14. N. Itagaki, S. Okabe, K. Ikeda, Prog. Theor. Phys. (Japan), Suppl. **142**, 297 (2001).
15. M. Seya, M. Kohno, S. Nagata, Prog. Theor. Phys. **65**, 204 (1981).
16. H. Horiuchi, K. Ikeda, Y. Suzuki, Prog. Theor. Phys. (Japan), Suppl. **52**, Chapt. 3 (1972).
17. E. Korkmaz *et al.*, Phys. Rev. Lett. **58**, 104 (1987).
18. E. Korkmaz *et al.*, Phys. Rev. C **40**, 813 (1989).
19. W. von Oertzen, to be published in Rev. Mod. Phys..
20. S. Okabe, Y. Abe, Prog. Theor. Phys. **61**, 1049 (1979).
21. D. Scharnweber, W. Greiner, U. Mosel, Nucl. Phys. A **164**, 257 (1971).
22. G. Herzberg, *Molecular Spectra and Molecular Structure* Vol. **I**: *Spectra of Diatomic Molecules* (Van Nostrand Reinhold, New York, 1950).
23. N. Soić *et al.*, Europhys. Lett. **34**, 7 (1996).
24. H.G. Bohlen *et al.*., Nuovo Cimento A **111**, 841 (1998).
25. H.G. Bohlen *et al.*, Prog. Part. Nucl. Phys. A **42**, 17 (1999).
26. D. Miljanić, N. Soić *et al.*, Fizika B **10**, 235 (2001).
27. H.G. Bohlen *et al.*, Phys. Rev. C **64**, 024312 (2001); R. Kalpakchieva, H.G. Bohlen, W. von Oertzen *et al.*, Eur. Phys. J. A **7**, 451 (2000).
28. H.G. Bohlen *et al.*, to be published in Phys. Rev.
29. M. Freer *et al.*, Phys. Rev. Lett. **82**, 1383 (1999).

30. M. Milin *et al.*, Europhys. Lett. **48**, 616 (1999).
31. M. Freer *et al.*, Phys. Rev. C **63**, 034301 (2001).
32. H. Horiuchi *et al.*, *Proceedings of the International Conference on Atomic and Nuclear Clustering, Santorini (1993)*, edited by W. von Oertzen, G.S. Anagnastatos (Springer, 1995); Z. Phys. A **349**, 279 (1994).
33. Y.K. Kanada-En'yo, H. Horiuchi, A. Ono, Phys. Rev. C **52**, 628 (1995).
34. Y.K. Kanada-En'yo, H. Horiuchi, A. Ono, Phys. Rev. C **56**, 1844 (1997).
35. Y.K. Kanada-En'yo, H. Horiuchi, A. Dote, Phys. Rev. C **60**, 064304 (1999).
36. Y.K. Kanada-En'yo, Phys. Rev. C **66**, 011303 (2002).
37. Y.K. Kanada-En'yo, H. Horiuchi, Phys. Rev. C **66**, 024305 (2002).
38. Y.K. Kanada-En'yo, H. Horiuchi, Phys. Rev. C **68**, 014319 (2002).
39. Y.K. Kanada-En'yo, H. Horiuchi, Phys. Rev. C **54**, R468 (1996).
40. Y.K. Kanada-En'yo, H. Horiuchi, Phys. Rev. C **55**, 2860 (1997).
41. Y.K. Kanada-En'yo, Phys. Rev. Lett. **81**, 5291 (1998).
42. N. Itagaki, S. Okabe, Phys. Rev. C **61**, 044306 (2000).
43. N. Itagaki, S. Okabe, K. Ikeda, Phys. Rev. C **62**, 034301 (2000).
44. P.A. Butler, W. Nazarewicz, Rev. Mod. Phys. **68**, 349 (1996).
45. N. de Takacsy, S. Das Gupta, Phys. Lett. B **33**, 556 (1970).
46. Y. Fujiwara *et al.*, Prog. Theor. Phys. (Japan), Suppl. **68**, 29 (1980).
47. W. von Oertzen, Phys. Lett. B **151**, 95 (1985).
48. L. Kraus, A. Boucenna, I. Linck *et al.*, Phys. Rev. C **37**, 2529 (1988).
49. Tsan Ung Chan, M. Agard, J.F. Bruandet, C. Morand, Phys. Rev. C **19**, 244 (1979).
50. Tsan Ung Chan, Phys. Rev. C **36**, 838 (1987).
51. F. Ajzenberg-Selove, Nucl. Phys. A **523**, 1 (1991).
52. S. Aroua, P. Navratil, L. Zamick *et al.*, Nucl. Phys. A **720**, 71 (2003).
53. W. von Oertzen, A. Vitturi, Rep. Prog. Phys. **64**, 1247 (2001).
54. P.R. Andrews *et al.*, Nucl. Phys. A **468**, 43 (1987).
55. M.E. Clark, K.W. Kemper, Nucl. Phys. A **425**, 185 (1984).
56. F. Ajzenberg-Selove, H.G. Bingham, J.D. Garrett, Nucl. Phys. A **202**, 152 (1973).
57. E.K. Warburton, W.T. Pinkston, Phys. Rev. **118**, 733 (1960).
58. S. Cohen, D. Kurath, Nucl. Phys. A **101**, 1 (1967).
59. H.U. Jäger, H.R. Kissener, R.A. Eramzhian, Nucl. Phys. A **171**, 16 (1971).
60. S. Lie, Nucl. Phys. A **181**, 517 (1972).
61. D.J. Millener, D. Kurath, Nucl. Phys. A **255**, 315 (1975).
62. H.T. Fortune *et al.*, Phys. Rev. Lett. **40**, 1236 (1978).
63. A.A. Wolters, A.G.M. van Hees, P.W.M. Glaudemans, Phys. Rev. C **42**, 2062 (1990).
64. M. Dufour, P. Descouvement, Nucl. Phys. A **605**, 160 (1996).
65. M. Yasue *et al.*, Nucl. Phys. A **509**, 141 (1990).
66. F.E. Cecil, J.R. Shepard, R.E. Anderson, R.J. Peterson, P. Kazckowski, Nucl. Phys. A **255**, 243 (1975).
67. H.J. Rose, O. Hausser, E.K. Warburton, Rev. Mod. Phys. **40**, 591 (1968).
68. H.T. Fortune, G.S. Stephans, Phys. Rev. C **25**, 1 (1982).
69. N. Vinh Mau, J.C. Pacheco, Nucl. Phys. A **607**, 163 (1996).
70. V.I. Krouglov, W. von Oertzen, Eur. Phys. J. A **8**, 501 (2000).
71. R.J. Peterson *et al.*, Nucl. Phys. A **425**, 469 (1984).
72. G. Kaschl *et al.*, Nucl. Phys. A **178**, 275 (1971).
73. W.R. Lozowski, Nucl. Instrum. Methods A **282**, 54 (1989).
74. N.M. Clarke *et al.*, J. Phys. G **14**, 1399 (1988).
75. J. Cook, M.N. Stephens, K.W. Kemper, Nucl. Phys. A **466**, 168 (1987).
76. M. Hamm, K. Nagatani, Phys. Rev. C **17**, 586 (1978).
77. J.C. Armstrong, W.E. Moore, A.G. Blair, Bull. Am. Phys. Soc. **4**, 17 (1959).
78. N. Anyas-Weiss *et al.*, Phys. Rep. C **12**, 201 (1974).
79. R.O. Lane *et al.*, Phys. Rev. C **23**, 1883 (1981).
80. R. Jahn *et al.*, Phys. Rev. Lett. **37**, 812 (1976).
81. R. Jahn *et al.*, Phys. Rev. C **18**, 9 (1978).
82. S. Mordechai *et al.*, J. Phys. G **4**, 407 (1978).
83. S. Mordechai *et al.*, Nucl. Phys. A **301**, 463 (1978).
84. F. Ajzenberg-Selove, E.R. Flynn, O. Hansen, Phys. Rev. C **17**, 1283 (1978).
85. D.B. Holtkamp *et al.*, Phys. Rev. Lett. **47**, 216 (1981).
86. D.B. Holtkamp *et al.*, Phys. Rev. C **31**, 957 (1985).
87. N. Soić, M. Freer, L. Donadille *et al.*, Phys. Rev. C **68**, 014321 (2003).
88. J.D. Brown *et al.*, Phys. Rev. C **38**, 1958 (1988).
89. R.B. Weisenmiller, N.A. Jelley, K.H. Wilcox, G.J. Kozniak, J. Cerny, Phys. Rev. C **13**, 1330 (1976).
90. T. Motobayashi *et al.*, Phys. Rev. C **34**, 2365 (1986).
91. D.A. Resler *et al.*, Phys. Rev. C **39**, 766 (1989).
92. H. Crannell *et al.*, Nucl. Phys. A **278**, 253 (1977).
93. R. Bijker, F. Iachello, Ann. Phys. (N.Y.) **298**, 334 (2002).
94. P. Navrátil, J.P. Vary, B.R. Barrett, Phys. Rev. Lett. **84**, 5728 (2000); Phys. Rev. C **62**, 054311 (2000); B. Barrett, Universites of Arizona, private communication, Krzyze Summerschool, Poland, September 2001.
95. D.J. Millener *et al.*, Phys. Rev. C **39**, 14 (1989).
96. H. Horiuchi, K. Ikeda, *Cluster Models and Other Topics* (World Scientific Publishing, Singapore, 1986) p. 65.
97. F.D. Snyder, M.A. Wagoner, Phys. Rev. **186**, 999 (1969).
98. W.-M. Wendler, M. Micklinghoff, Nucl. Phys. A **436**, 477 (1985).
99. R.L. McGrath, Phys. Rev. **145**, 802 (1966).
100. M.A. Plum *et al.*, Phys. Lett. B **137**, 15 (1984).
101. M.A. Plum *et al.*, Phys. Rev. C **40**, 1861 (1989).
102. H. Horiuchi, K. Ikeda, Prog. Theor. Phys. (Japan) **40**, 277 (1968).
103. J.P. Lowe, *Quantum Chemistry*, 2nd edition (Academic Press, New York, 1997) pp. 202-213.
104. A.N. Andreyev, M. Huyse, P. Van Duppen *et al.*, Nature **405**, 430 (2000).